Mandibular biomechanics as a key factor to understand diet in mammals

Jordi Marcé-Nogué

Introduction

The mammalian mandible plays a fundamental role in food processing, as it transmits the forces generated by masticatory muscles to the food through the teeth (Maynard-Smith & Savage 1959). Generally speaking, the greater the forces required to fracture ingesta, and the more often such forces are needed, the stronger the mandible has to be to maintain its structural integrity (Hogue 2008). In that line, it has been suggested that among primates, those that include hard-food in their diets have stiffer mandibles when compared to soft-food eaters (Marcé-Nogué et al. 2017b). However, other attempts to establish relationships between mandibular morphology and dietary categories have not been particularly successful (Ross et al. 2012). If the latter is true and biomechanics cannot be used to establish relationships between morphology and function, it has been argued that it is probably because these biomechanical analyses are flawed or incomplete, or that non-mechanical factors such as phylogeny are more important determinants of morphology (Ross & Iriarte-Diaz 2014). Nevertheless, there is a general consensus that trying to understand the interaction between the mammalian feeding mechanism and the processed ingesta represents a unique opportunity for the study of ecomorphological adaptations in extant species, as well as having the potential to acquire valuable tools for the reconstruction of oral behaviors in extinct taxa. Hence the importance of this particular topic.

The association between dietary preferences and biomechanical performance has traditionally been studied as the relationship between dental and mandibular morphology (Fig. 4.1). For example, carnivorous mammals have carnassials that act as blades allowing enlarged and often self-sharpening edges to pass by each other in a shearing manner. Herbivorous ungulates have developed reduced canine teeth and specialized molars to grind fibrous food by lateral movements. Among other examples, primates have teeth that exhibit an elaborated cusp pattern of the molars that crush the food (Kardong 2014).The way teeth work (e.g. blading, grinding, or crushing) is adapted to the diet as well as the morphology of the mandibles, thus enabling the generation of different models of distribution and position of the muscular forces and bite positions based on different geometries (Vizcaíno et al. 2016). The influence of muscular forces on the design of the shape of the mandible (e.g., Sella-Tunis et al. 2018 in humans), as well as the influence of the position of the condyle allowing different mandible movements (Maynard-Smith & Savage 1959) are evidence that reinforces the idea that food is processed differently depending on mandibular morphology.

For these reasons, feeding biomechanics represents the set of analyses performed to "[…] relate variation in feeding system morphology (size and shape of muscles, bones, teeth, tongues or joints) to variation in how animals feed (feeding behavior) and what they feed on (diet)." (Ross & Iriarte-Diaz 2014: 105). This relationship between muscular and bite forces, mandibular size and shape, and the consumed ingesta have previously been studied in the mandibles of different mammalian clades such as terrestrial Cetartiodactyla (Christiansen & Wroe 2007, Hogue & Ravosa 2001, Spencer 1995, Varela & Fariña 2015), Chiroptera (Freeman 1979, 1981, 1984, 1988, 2000), Primates (Bouvier 1986a,b, Taylor 2006) and Carnivora (Biknevicius & Ruff 1992, Radinsky 1981a,b). These works used classical biomechanics based on the laws of static mechanics and beam theory, hence not requiring the application of computer simulation techniques to model complex biological geometries, thus avoiding a high computational cost.

The eruption of computational methods opened a whole array of new possibilities to investigate feeding biomechanics. Specifically, computational biomechanics represents the application of engineering computational tools, such as the finite element analysis (FEA) (Zienkiewicz & Taylor 1981) to study the mechanics of biological systems. Computational models and simulations are particularly useful to predict the relationship between parameters that are otherwise challenging to test using experimental approaches and are also quite helpful when designing more relevant experiments, hence reducing the time and costs of such tests. The underlying premise of the method is that a complex geometry can be subdivided into a mesh consisting of a number of finite elements in which the respective mechanical equations are approximately solved. Although FEA (see Rayfield 2007 for a review) or multibody dynamic analysis (see Curtis 2011 for a review of MDA) have been common approaches in engineering and biomedicine for more than thirty years, they have also been applied to biological research in order to address questions related to biomechanics and the evolution of living and extinct vertebrates (using both 2D or high-resolution 3D models). Vertebrate paleontologists have also applied complementary non-invasive techniques, such as computed tomography (CT), which is a useful tool to generate accurate 3D images of living structures in a reverse engineering process, thus facilitating the application of computational biomechanics. The reliability and bio-fidelity of the biomechanical models has increasingly improved by capturing the real geometries of the specimens under analysis. Previous approaches

T. Martin & W. v. Koenigswald (eds.): Mammalian Teeth – Form and Function. Pp. 54–80, 13 figs., 8 tabs.

DOI: http://doi.org/10.23788/mammteeth.04 Published 22 December 2020

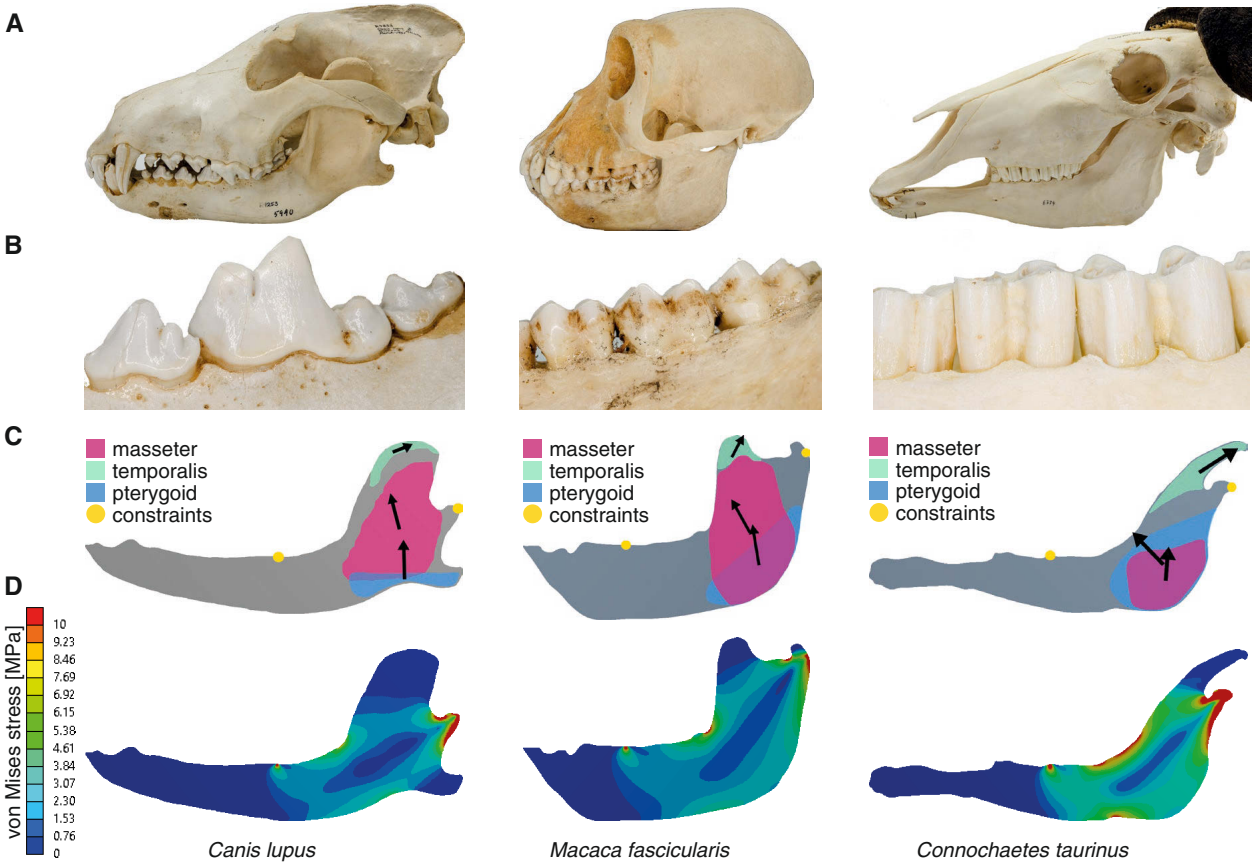

Fig. 4.1. Morphology and bite forces in mammalian crania and mandibles. **A,** cranium and mandible; **B,** details showing different tooth morphologies; **C,** free-body diagram of the biomechanical problem of the mandible during chewing; **D,** von Mises stress results after a finite element analysis of three different taxa: *Canis lupus* (carnivore), *Macaca fascicularis* (primate) and *Connochaetes taurinus* (ungulate). Not to scale.

relied on simplified lever or beam models, which although still useful, possess many known limitations that can be overcome by modern computational biomechanics.

To date, FEA has been conducted in a wide spectrum of vertebrates providing new insights into biomechanical function, particularly regarding the constraints and adaptive values of certain morphologies and bone structures. These bony structures are generally considered to be a force transmission system that can be studied by mean of mechanics laws. For instance, the biomechanics of the mandible in different mammalian families has been studied using FEA to obtain the state of stresses during mastication in 3D models (Gill et al. 2014, Gröning et al. 2011b, Lautenschlager et al. 2018, Püschel et al. 2018, Tseng & Binder 2010, Zhou et al. 2019), as well as using simplified planar models (Fletcher et al. 2010, Marcé-Nogué et al. 2017b, Neenan et al. 2014, Piras et al. 2013, Serrano-Fochs et al. 2015). Other studies have approached this problem including the study of both the skull and the mandible (Dumont et al. 2011, Strait et al. 2013, Tseng 2013, Veitschegger et al. 2018). Nonetheless, it is important to keep in mind that if a study aims to detect dietary preferences, it would be preferred to analyze mandibles as part of the antagonistic system, since the lower jaw may be more susceptible to failure than the cranium (Wroe et al. 2010), and also because cranium morphology is influenced by several other non-feeding variables (Tseng & Flynn 2018). In fact, it has been noted that cranial shape reflects a compromise between several diverse functions (e.g., phonation, cognition, respiration), which could mask a strong dietary signal (Püschel et al. 2018). By contrast, the mandible is primarily involved in food acquisition and consumption, and consequently it is to be expected that its morphology better reflects ingesta-related adaptations (Gröning et al. 2011b).

It is logical to wonder how paleontologists and paleoanthropologists have applied these biomechanical tools in fossil taxa, taking into account that many variables are unknown and impossible to obtain from skeletal morphology alone. The answer is relatively simple. If it is possible to study extant species that are phylogenetically related and/or share the same or similar diet to the fossil taxa of interest, and if it is possible to find correlations, associations or differences to their dietary preferences or their ingesta characteristics, then it would be possible to study the biomechanics of the fossil taxa and find the appropriate relationships with the biomechanical data. Nonetheless, there are two important questions that need to be addressed before carrying out analyses on fossil specimens. These questions are related to the intrinsic nature of biological data and make the study of biological structures completely different to the more common mechanical problems solved by engineers in other fields. The first one is variation, which focuses on how different models are properly compared when considering both intra and inter species variability. This means that it is necessary to create an appropriate comparative

framework where a large number of different models and data can be analyzed and compared. The second one is how to post-process the extremely large amount of data derived from FEA results or classical biomechanics in a quantitative way that allows the obtained data to be used and combined with statistics, geometric morphometrics, phylogenetic models or even machine-learning algorithms to try to find affinities between the feeding behavior and the diet of the taxa.

Consequently, the aim of this chapter is to discuss classical and computational biomechanics of the mandible in the study of dietary adaptations in mammals. Firstly, a brief theoretical background in mechanics will be provided to facilitate understanding of the concepts used in this chapter. Afterwards, these concepts will be used in examples of biomechanics of the mandible. Secondly, the use of FEA in mammalian mandibles will be discussed, along with the concept of a comparative framework that enables the comparison of different models, as well as reviewing the latest methods to quantify and compare a large number of FEA models. Finally, an example using different mandibles of armadillos will be provided and discussed to further develop the understanding of the topics under discussion. This will provide insights about the connection between mandibular biomechanical performance and dietary preferences.

Brief introduction to biomechanics

Theoretical background

Biomechanics is the study of the structure and function of the mechanical aspects of biological systems, at any biologically relevant organization level, from whole organisms to small cells, using the methods of mechanics (Alexander 2005). By contrast, mechanics is a more general field of science concerned with the behavior of any physical body subjected to forces or displacements.

Biomechanics comprises several sub-areas, such as for example aerodynamics to study the flight of birds and insects, hydrodynamics to study how fish swim, locomotor mechanics to study how animals move, as well as the study of chewing mechanisms using static theory, among other sub-fields. Statics is the branch of mechanics that is concerned with the analysis of loads acting on physical systems that are in static equilibrium with their environment. It means that a body is in static equilibrium when it fulfils the first condition for equilibrium, which requires that the net force applied to the system must equal zero, as well as the second condition for equilibrium, meaning that the net torque applied to the system must also be zero. This is the application of Newton's second law when the body has a null acceleration.

Newton's three laws of motion are physical laws that, taken together, constitute the basis of classical mechanics.

- First law: An object in uniform motion remains in that state of motion unless an external force is applied to it.
- Second law: The vector sum of the external forces F on an object is equal to the mass of that object multiplied by the acceleration vector of the object.
- Third law: When one body exerts a force on a second body, the second body simultaneously exerts a force equal in magnitude and opposite in direction against the first body. They are called action force and reaction force.

Newton's laws describe the relationship between a body and the forces acting upon it. Therefore, they are the base of any biomechanical model, both classical as well as the computational ones.

Free-body diagram. A free-body diagram (FBD) is a graphical illustration which is used to visualize the applied forces, movements, and resulting reactions on a body in a given condition or mechanical scenario. They depict a body or connected bodies with all the applied forces and moments, as well as reactions that act on that/those bodies. An FBD is an important step in understanding statics, dynamics and other forms of classical mechanics, because is not meant to be a scaled drawing. It is a diagram that is modified as the problem is solved.

A free body diagram explicitly excludes some things: (1) Bodies other than the free body (2) Constraints; the body is not free from constraints; constraints have just been replaced by the forces and moments that they exert on the body (Newton's third law) (3) Forces exerted by the free body (supported by Newton's third law) (4) Internal forces and (5) in the case to solve a dynamic problem, the velocity or acceleration vectors.

Lever mechanics. Lever mechanics are based on Newton's laws and the condition for static equilibrium of statics. A lever is a body connected to a fixed point by a hinge or pivot called fulcrum and obeys the following physical law: the ratio of output to input force is given by the ratio of the distances from the fulcrum to the points of application of these forces.

Lever mechanics is useful in the context of chewing biomechanics, when studying the effect of muscles of the mandible on the bite force. There is a parameter called mechanical advantage (MA, equation 1) that is a measure of the force amplification achieved by using a mechanical system and is defined as the ratio of the force produced by the mechanical system (F_{output}) to the force applied to it (F_{input})

$$MA = \frac{F_{output}}{F_{input}} \qquad \text{(equation 1)}$$

This parameter is useful because it is a dimensionless proportion (or ratio) of forces and, consequently, is not related to the size of the system. It allows to compare models without the influence of size on the results.

Elasticity: Stress and strain. Up to this point we have presented the concepts of biomechanics without considering what is happening inside the analyzed bodies, and without taking into consideration the effect of the forces on the deformation of a body. All the bodies in our surroundings experience deformations. For instance, there could be small

deformations that we cannot see in concrete buildings, or there might be larger deformations in rubbers, such as in the case of a chewing gum.

In physics, elasticity is the ability of a body to resist reversible deformations when it is under the action of external forces, and to return to its original size and shape when that force is removed. Although solid objects will deform when adequate forces are applied to them, it is important to bear in mind that perfect elasticity is only an approximation of the real world because few materials remain purely elastic, even after very small deformations.

When we want to study what is happening inside a body, and how this body deforms under the application of a load, we need to study the laws of elasticity using the methods of continuum mechanics (Mase & Mase 1999). Continuum mechanics is a branch of mechanics that studies the mechanical behavior of materials when they are modelled not as discrete particles but as a continuous mass.

In biomechanics, bony structures can be considered bodies modelled as a continuous mass with small deformations, which means that one can apply to them all the equations derived from continuum mechanics and the linear theory of elasticity. Other biological structures such as soft tissues, are beyond the scope of this chapter and should be analyzed using non-linear theories.

When studying continuum mechanics, two concepts of great interest need to be mentioned, namely stress and strain. Stress is a quantity that corresponds to the internal forces that adjacent particles of a continuous material apply on each other. Stress is computed in a specific plane of the body and it is equivalent to the force divided by the surface of this plane. Strain is the ratio of the deformation of the material. It is computed as the proportion of displacement when a body is deformed with the original dimension of the body. Both are commonly used in biomechanics to study what is happening inside a body subjected to external loads.

$$\sigma = \frac{F_x}{S}\left[\frac{N}{mm^2}\right] \qquad \text{(equation 2)}$$

$$\varepsilon = \frac{x}{l}\left[-\right] \qquad \text{(equation 3)}$$

Where σ is the stress, F is the force, S the surface, ε the strain, x the distance of the elongation and l the original length of the bar (Fig. 4.2A). Compression or traction are obtained depending on how the balanced forces are applied (i.e. inwardly or outwardly) (Fig. 4.2B).

In general, stress and strain are computed in a specific point of the body in relation to a perpendicular plane and may be regarded as the sum of two components: the normal stress (compression or tension) perpendicular to this plane (Fig. 4.3A), and the shear stress that is parallel to this plane surface (Fig. 4.3B). Note that, for one point it is possible to define infinite normal and shear stress as function of the perpendicular plane in which they are computed (see tensorial notation below for further explanation).

$$\sigma = \frac{F_x}{S}\left[\frac{N}{mm^2}\right] \qquad \text{(equation 4)}$$

$$\tau = \frac{F_y}{S}\left[\frac{N}{mm^2}\right] \qquad \text{(equation 5)}$$

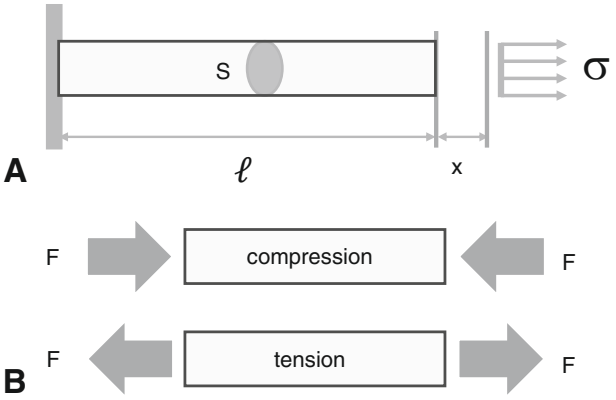

Fig. 4.2. Stress and strain. **A,** parameters of the definition of stress and strain and **B,** definition of tension and compression.

In linear elasticity, stress and strain are related via the Hooke's law that links both variables by means of the Young's modulus. E is the Young's modulus, a mechanical property of linear elastic solid materials. Constitutive equations are used to relate two physical quantities that are specific to a material and that describe the response of that material to external inputs such as applied fields or forces. They are combined with other equations governing physical laws to solve physical problems; the relationship between applied stresses to strains is a linear constitutive equation because the relationship between them is linear and proportional to the Young's modulus. Other materials such as soft tissues use other constitutive equations because they do not follow linear elasticity. For bones, the use of Hooke's law is quite common (Doblaré et al. 2004).

$$\sigma = E \cdot \varepsilon \qquad \text{(equation 6)}$$

The Poisson coefficient is the ratio of transverse contraction strain to longitudinal extension strain in the direction of stretching force. It measures the Poisson effect, which is the phenomenon that happens when a material tends

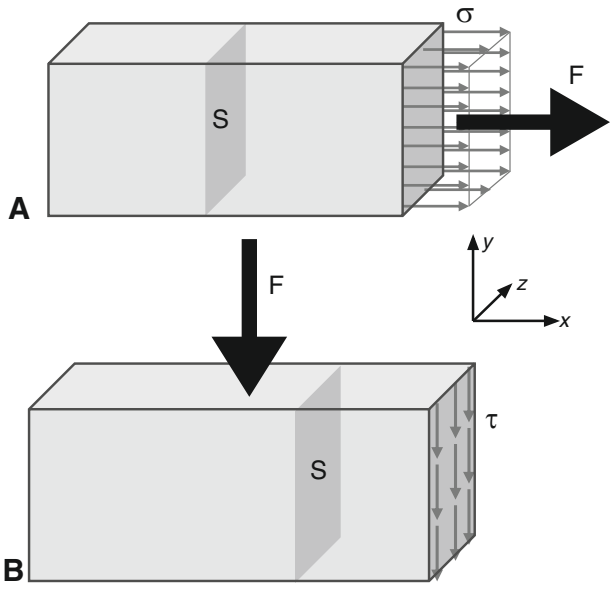

Fig. 4.3. Normal and shear stress. Definition of **A,** normal stress and **B,** shear stress, where F are the forces in the xyz coordinate axis and S is the surface.

to expand in directions perpendicular to the direction of compression or conversely, tends to contract if the material is stretched. This value is also necessary when defining the constitutive equation of the Hooke's law in two or three dimensions.

Beam mechanics. Classical beam theory is a simplification of the linear theory of elasticity that provides a way of calculating the loads and deflection of beams when they are subjected to outer forces. The main difference between lever mechanics and beam theory is that levers are not deformable whilst beam theory assumes the deformation of the body under study. Another important difference is that in lever mechanics only Newton's laws are used to solve the input and output forces whereas in beam theory, the use of the Newton's laws is needed to get the input and output forces and then the stresses and strains inside the beam. For this reason, a beam is a mechanical prism: a line with an associated cross-section where we calculate the stresses. It covers the case of small deflections of a beam that are subjected to lateral loads only. Moreover, Hooke's law is achieved between stresses and strains and plane sections keep on the plane after deformation. This means each cross-section of the beam is always at 90 degrees to the line that describes the beam (Timoshenko 1955).

Once we know the value of the input (actions) and output forces (reactions) solved by Newton's laws, the force that each cross-section of the beam is dealing with, is computed via force and moment laws keeping the equilibrium of forces in all the cross-sections. The equations of the forces and moment laws depend on the position of the section along the beam. They can be graphically displayed with force and moment diagrams to facilitate the interpretation. For example, a force applied in a specific point can vary its action in the cross-section due to the distance from this point creating a bending moment. The forces applied in the beam can create compression/tension, bending, shear and torsion.

The stresses (both normal and shear) in the cross-section of the beam depend on whether they are from compression/tension, bending, shear, and torsion or if they are linearly related with the forces applied via the Navier equations for bending, the Collignon theorem for shear, or the torsion equations (Timoshenko 1955). The diagrams are a good option to understand in which points the effects of the forces are higher in order to correlate them with anatomical or functional aspects (see the example below). In this case, the most important thing to consider is that the normal stress produced by the bending moment is parallel to the direction of the beam. If we decide that the axis of the beam is the x axis, then the normal stress is σ_x (see tensorial results below). And the shear or torsion stress are also lying on the plane of the cross-section.

Another important issue is that the transformation of shearing and normal forces, as well as bending and torsional moments to the stress values implies the geometrical definition of the beam's section. In structural mechanics, beams are easy to define because they have simple geometries, but when used in biological systems some simplifications need to be assumed. Mandibles can be modelled as hollow tubes (Porro et al. 2011) or the real cross-sectional properties at some locations of the model can be calculated following the method described by Cuff & Rayfield (2013).

In the above-mentioned examples, stress was measured for bending moments. Torsion, compression, or shear can also be studied using beam models. In this case, other diagrams must be obtained instead of the bending diagrams, and other equations (instead of Navier's) are needed to relate the diagram to stress values. All these equations to transform the results from beam theory to stress require the definition of the geometric properties of the section of the beam. In this case the beam is the mandible. A good example to understand the implications of these simplifications in the mammal jaw can be found in van Eijden (2000).

Classical biomechanical methods applied to mammalian mandibles

Three examples are presented here in which the authors have used classical biomechanics. The two first examples by Maynard-Smith & Savage (1959) and Crompton & Parkyn (2009) are based on lever mechanics to study mechanical advantage, whereas Thomason (1991) used beam theory.

Firstly, Maynard-Smith & Savage (1959) studied the biomechanics of the mandible of one carnivore (*Martes)* and one artiodactyl (*Strepsiceros*). They analyzed the efficiency during chewing via the mechanical advantage of these two taxa which feed in different ways and have different mandibular shapes. The models included the temporalis and the masseter muscular forces, as well as the bite force of the canines. A reaction force appeared on the articulation point in the glenoid fossa. They found big differences between the mechanical advantage of the temporal and masseter muscles in the carnivore and the herbivore. These differences were associated with the different geometries of the lower mandible to perform a high MA in relation to the jaw closing muscles. In the case of the carnivore, the temporalis muscle presents the higher MA because the lever arm (the distance to the articulation point) is higher. This corresponds to the muscle that allows the mandible to open in the sagittal plane creating a big and powerful bite without dislocating the mandible. In contrast, in *Strepsiceros* the masseter presents a higher MA because the lever arm is higher for the masseter. This is the muscle that allows the mandible to move laterally and antero-posteriorly making the grinding of herbivorous food possible. Therefore, the different geometries of the two mandibles and the position of the articulation point play an important role in the value of the MA, as well as for the efficiency of chewing.

By using lever models, Crompton & Parkyn (2009) studied the lower mandible of Triassic mammals in which both the reptilian and mammalian mandible articulations were defined. The models included the resultant forces of jaw closing muscles (temporalis, masseter, and pterygoid) and the bite force and the reaction force in the articulation thrust. They demonstrated how the component parts of the mandible musculature gradually changed their orientation (due to the changes in their geometry), in such a way that the reaction force to which the jaw joint was subjected in the articular thrust (the fulcrum of the lever) was progressively decreased whereas there was an increase in the bite force across the post-canine teeth.

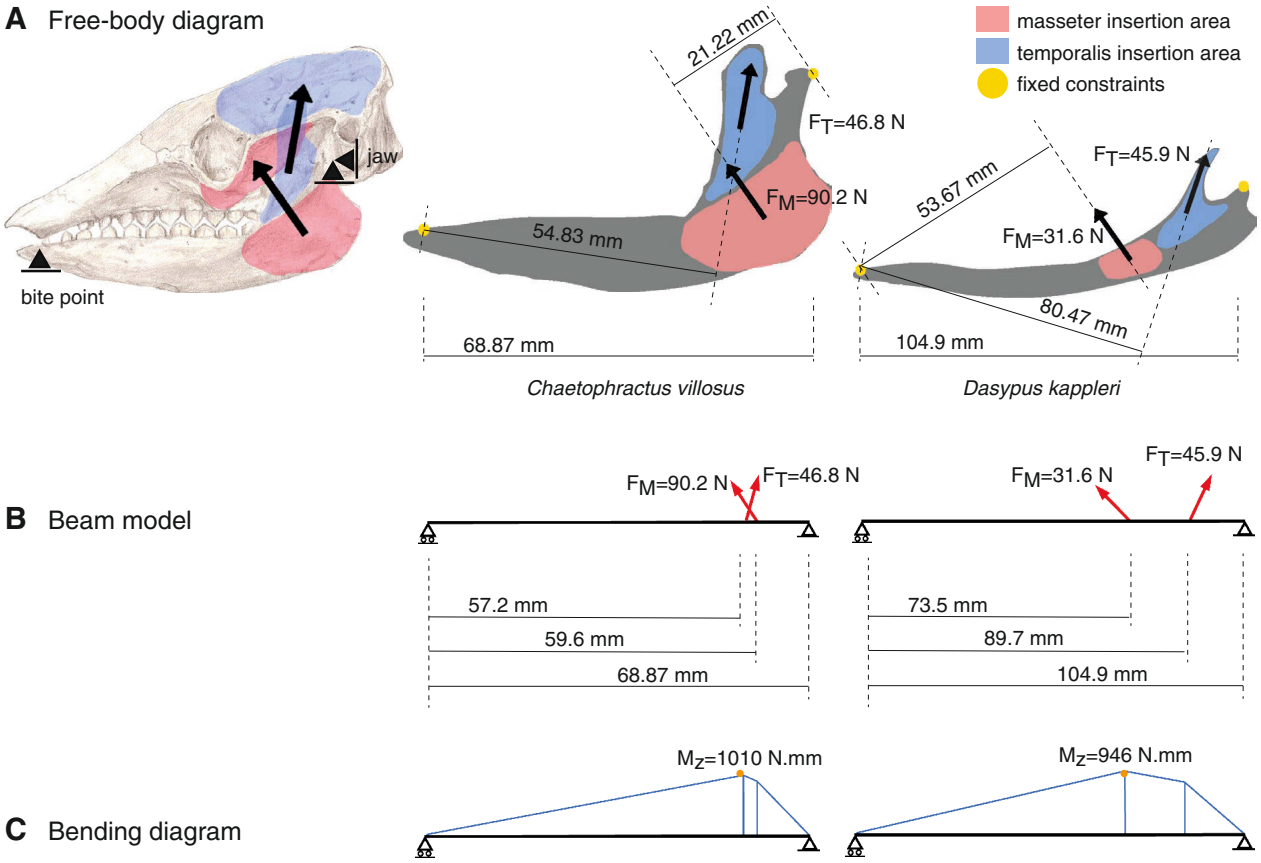

Fig. 4.4. Bite force diagrams of armadillo mandibles. **A,** free-body diagram of a bilateral bite using a two-dimensional approach; **B,** beam model; **C,** bending diagram of *Chaetophractus villosus* and *Dasypus kappleri* from Serrano-Fochs et al. (2015).

Finally, Thomason (1991) modeled the skull of Canidae and Felidae as tubular beams formed by the facial and neurocranial regions, with the attached 'jug handles' of the zygomatic arches. In that case, the model included the reaction force at the articulation thrust and the muscular forces from the masseter and the temporalis. The bite force was studied in two cases: on the canine and on the molar positions. The authors wanted to test the hypothesis that the bending strength of the skull in some mammals correlates with the maximal loads imposed through the masticatory apparatus. The application of the beam theory allowed to assess the cranial strength during bending and, for instance, the Navier-Bernouilli equation was used to relate muscle and bite forces with the stresses inside the skull. In that case, the author used between 20 and 30 transverse CT scan sections through each skull to calculate the cross-sectional properties for the equation. This is one of the first works to show that bending stresses might be of importance in the cranial design of mammals and also has set the stage for more detailed future modelling.

Practical example A. Two different armadillos are studied: *Dasypus kappleri* and *Chaetophractus villosus*, each one presenting different dietary preferences. *D. kappleri* is a generalist insectivore, whereas *C. villosus* has an omnivore diet. The free-body diagram of the mandible, including masseter and temporalis muscle forces, is shown in Figure 4.4. Fixed positions are located on the bite position and on the jaw joint, thus constraining both directions on the jaw-joint and the vertical displacement on the bite point.

Muscle forces are calculated using muscle areas, and a value of 0.3 MPa (force per unit area) is assumed as muscular contraction. This value, estimated by Alexander (1992), has been considered in several works as a valid estimate for the isometric contraction of each adductor muscle (Thomason 1991). In this example, we assumed that the insertion area of the muscle is a good proxy of the 3D muscle cross-section, thus enabling the computation of muscular forces.

Equilibrium of forces in the free-body diagram: According to the equations of equilibrium of forces and the condition for static equilibrium of the statics, the bite force – applying the equilibrium of moments in the jaw joint – can be solved using equation 7. Results can be found in Table 4.1. F_M and F_T are the forces of the masseter and temporalis, l_M and l_T the lever arms of the masseter and the temporalis and l_{Total} the length between the bite point and the jaw joint.

$$BF = \frac{F_M \cdot l_M + F_T \cdot l_T}{l_{Total}} = \frac{0{,}3 A_M \cdot l_M + 0{,}3 A_T \cdot l_T}{l_{Total}}$$

(equation 7)

The results from classical biomechanics using the free-body diagram show that *Chaetophractus villosus* generates a higher bite force and possesses a more efficient mechanical advantage. This higher biomechanical performance allows *Chaetophractus villosus* to eat a more demanding

omnivore diet, whereas *Dasypus kappleri* probably does not need to perform a high bite force in order to crush insects before processing them.

Beam theory in a linear model: The use of the beam theory enables to find the maximum bending moment in the mandible by assuming that mandibular morphology can be represented as a straight line (Fig. 4.4). Curiously, both *Dasypus kappleri* and *Chaetophractus villosus* present similar values of maximum bending moment (1010 and 946 N·mm respectively) but this does not mean that there is a lack in functional differences, because the capacity to withstand this bending moment exclusively depends on the design of the mandible. According to Serrano-Fochs et al. (2015), the mandible of *Chaetophractus villosus* is thicker (5 mm vs. 3.5 mm) and the body of the mandible is broader than that of *Dasypus kappleri*. The corpus of the mandible of *Dasypus kappleri* is narrow in height and limiting its capacity to sustain the stresses derived from the bending moment. These results from beam models clearly suggest that *Chaetophractus villosus* is capable to withstand higher bending moments than *Dasypus kappleri* when chewing, therefore also is capable to process more demanding diets such as an omnivore one.

There is a difference between using the free-body diagram and the beam-model which explains the different bite force values (see Tab. 4.1 and 4.2 for the two approaches). The geometry assumed in both cases is different. In the free-body-diagram, the distances used from the muscles to the bite point and the condyle are based on the actual geometry, whereas in a beam model the position of the forces is in the line defined by the beam. This changes the values of the distances, and consequently, the value of the bite force. The free-body diagram is better suited to study muscle and bite forces, whereas the beam model allows the study of stresses in the cross-sections.

From the values of the maximum bending moment and from geometrical properties of the section of the mandible, normal stress values in the mandible can be found using the Navier equation (equation 8). In this example, we will assume a hollow ellipse as a constant cross-section of the mandible, and the second moment of inertia is obtained via equation 9.

$$\sigma_{xx} = \frac{M_Z}{I_Z} \cdot y = \frac{M_Z}{\frac{\pi(ab^3 - a_1 b_1^3)}{64}} \cdot \frac{b}{2} \qquad \text{(equation 8)}$$

$$I_Z = \frac{\pi(ab^3 - a_1 b_1^3)}{64} \qquad \text{(equation 9)}$$

Where M_z is the bending moment computed in the beam, I_z the second moment of inertia in the axis of the bending and y the distance from the centroid of the section to the point of the section under study.

High stresses are in the farthest point from the center of the cross-section during bending. Geometrical parameters of the section are described in Table 4.3 assuming, for this example, a constant cortical bone thickness of 1 mm in both models. The geometric parameters a, a_1, b, and b_1 are defined in Table 4.3 and are real measurements from the models (Serrano-Fochs et al. 2015). The normal stress obtained using equations 8 and 9 for both mandibles assuming a beam model (Tab. 4.3) also supports that the mandible of *Chaetophractus villosus* is stronger than the one of *Dasypus kappleri* during chewing.

Table 4.1. Results from equilibrium of forces.

Taxon	Masseter area (mm^2)	Temporalis area (mm^2)	Masseter force (N)	Temporalis force (N)	Bite force (N)	Mechanical advantage (MA)
Dasypus kappleri	105.37	153.18	31.6	45.9	15.66	0.2
Chaetophractus villosus	300.58	156.08	90.2	46.8	34.97	0.25

Table 4.2. Results from beam theory.

Taxon	Masseter area (mm^2)	Temporalis area (mm^2)	Masseter force (N)	Temporalis force (N)	Bite force (N)	Mechanical advantage (MA)	Mz max (N·mm)
Dasypus kappleri	105.37	153.18	31.6	45.9	12.87	0.16	−1010
Chaetophractus villosus	300.58	156.08	90.2	46.8	17.63	0.13	946

Table 4.3. Reometrical parameters for the mandibles of *Dasypus kappleri* and *Chaetophractus villosus* when assuming a beam with a hollow elliptic cross-section.

Taxon	a (mm)	a_1 (mm)	b (mm)	b_1 (mm)	I_z (mm^4)	Mz (N·mm)	σ_x (N·mm^2)
Dasypus kappleri	3.51	0.51	8	6	82.81	1010	48.8
Chaetophractus villosus	4.94	2.94	12	10	274.71	946	20.7

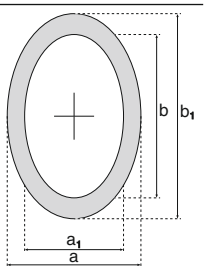

Finite element analysis in mammalian mandibles

Brief introduction to finite element analysis

The finite element analysis (FEA) is a non-invasive computer simulation technique used in engineering. It uses the numerical technique of the finite element method (FEM) to solve the equations of continuum mechanics by dividing a geometry into a finite number of discrete elements known as a mesh (Kupczik 2008) to which the equations are applied. Mechanical properties of these elements are defined in order to give the structure a realistic behavior. The model is constrained to anchor it in space and includes the external forces applied to it. FEA is used to solve the equations of the elasticity in a deformable body under the effect of external forces.

FEA and beam theory are two different approaches to solve the same mechanical problem, yet with the limitation that beam theory can be exclusively used when assuming linear geometries with cross-section, whereas FEA can be applied to any geometry. The equations of lever mechanics based on Newton's Laws are included when solving a mechanical problem in both FEA and beam theory. They are also solved when these methods are used. Therefore, beam theory and FEA can also solve reaction forces but it makes no sense to use these approaches to exclusively calculate these external forces, since they can be solved by hand using Newton's laws (Sellers et al. 2017, Snively et al. 2015).

In mammalian mandibles, FEA enables the observation of stress distribution patterns of the specimens by simulating loadings and forces involved in the masticatory function. Under equivalent loads, these stress patterns can be interpreted as a sign of the relative strength, with higher stress indicating a weaker mandible. Assuming that more robust or stronger mandibles would be needed both for processing harder food items, these mandibles should be expected to be weaker (i.e., displaying higher stress levels) than those belonging to animals feeding on harder items, such as nuts, shells or bones. On the other hand, differences in the stress distribution pattern may give a clue regarding different aspects of the feeding ecology of the analyzed species.

There are several types of FEA depending on the nature of the geometry imported. A three-dimensional geometry e.g., from a CT-scan implies the use of three-dimensional solid models; a two-dimensional geometry requires the solution of a planar model using the equations of plane elasticity. Surface geometries in a 3D space require the use of shell models, whilst geometries based on lines need the use of linear elements. The latter is the exact computational translation of beam theory.

It is usual to model mammal mandibles as three-dimensional solid models (Gill et al. 2014, Gröning et al. 2011b, Püschel et al. 2018, Tseng & Binder 2010) or to represent them as simpler planar models (Fletcher et al. 2010, Marcé-Nogué et al. 2017b, Piras et al. 2013, Serrano-Fochs et al. 2015). In continuum mechanics, plane elasticity makes reference to the study of particular solutions of the general elastic problem in bodies that are geometrically mechanical prisms (that is, an area with a constant thickness) (Mase & Mase 1999). In particular, a plane stress solution occurs in structural elements where one dimension (the thickness) is very small compared to the other two, and the stresses are negligible with respect to the smaller dimension.

Steps to perform a finite element analysis

Geometry of the model. Models of mammalian mandibles can be obtained from the digitalization of real specimens by using CT-scans, photogrammetry or similar digitalization techniques that can register morphologies in three-dimensions and in full detail (see review in Cunningham et al. 2014). Another option is to generate them from scratch based on photos or other templates in CAD software (see Rahman & Lautenschlager 2016 for the box modelling approach).

The advances in computational tools to perform virtual reconstruction and restoration techniques of the original morphology of fossils, enable the creation of accurate and realistic three-dimensional models (Lautenschlager 2016). In all cases, during the reconstruction process, irregularities in the surface due to the generation of the model from the CT scanner need to be repaired using refinement and smoothing tools (Marcé-Nogué et al. 2011).

Planar models can be created from published photographs or built from scratch. In order to take the photographs in the most consistent way, some procedures need to be carried out in order to standardize images (de Esteban-Trivigno 2011), and then the use of CAD software allows the creation of models based on splines which are traced on the picture (see Fortuny et al. 2010 and Serrano-Fochs et al. 2015 for the full methodology).

Material properties. Bone is a rigid organ that forms part of the vertebrate skeleton. The hard and dense outer layer is composed of cortical bone tissue. Trabecular bone tissue corresponds to the internal tissue of the skeletal bone, being an open cell porous network. The mechanical properties of a particular bone depend on both composition and structure, which are fundamental parameters to be considered when simulating the behavior and response of a model when loads are applied. Although composition is not constant in living tissues, it is normally assumed (for simplicity and computational costs) that the mechanical properties of cortical and trabecular bone depend on apparent density and mineral content (see Doblaré et al. 2004 for a review).

The difficulties in modeling bone material properties in FEA models have driven researchers to assume isotropic behavior and to consider that bone, like most biological materials, is elastic and fails under a ductile model of fracture (Nalla et al. 2003). Isotropy means that the properties are taken to be the same in all directions, whereas anisotropy means having different properties in different directions. Orthotropy is present when the material

properties differ along the three orthogonal axes. Another common assumption of most FE analyses in the literature is to consider the mechanical behavior of bone (trabecular and cortical) as being linear, which is usually an accurate enough assumption (Doblaré et al. 2004). This means that the relationship between stress and strain is proportional and the constitutive equation of linear elasticity based on Hooke's law can be assumed. This also implies that using Young's modulus and Poisson coefficient is enough to characterize bone. Cortical bone is stiffer and, therefore, has a higher Young's modulus than trabecular bone.

One of the main problems when working with animal bones – and especially with fossil taxa – is the absence of material data to define Hooke's law (Young's modulus and coefficient of Poisson). This problem is normally tackled by using data available from closely related species, or from species with similar bone structure. The use of appropriate material properties depends on the available information from phylogenetically or ecologically related taxa. It is important to bear in mind that modelling other materials such as soft tissues, implies the application of non-linear constitutive equations, which in turn results in more computation time, (i.e., solutions mostly based on the equations of hyperelasticity). A hyperelastic material is a type of constitutive model of an ideally elastic material for which the stress-strain relationship derives from a strain energy density function that does not follow a linear relationship. It is common to use these constitutive models in FEA for ligaments (Qian et al. 2009), cartilage (Gislason et al. 2017), or arteries (Early et al. 2009) but not when analyzing osteological structures, such as mandibles.

Biting scenarios. Different biting scenarios have been used to study the chewing mechanism of mammals. According to Preuschoft & Witzel (2002), the skull of mammals can be loaded in three different ways: (1) assuming the weight of the head and prey or food acting downward on the mandible, (2) applying arbitrary forces or movements in the plane of the tooth row that create movements of the prey in relation to the head (defined as extrinsic loads by McHenry et al. (2007), and (3) applying the adduction of the mandible via the muscle forces which leads to reaction bite forces in the teeth (defined as intrinsic loads by McHenry et al. 2007). The cases with intrinsic loads can be modelled at the different tooth positions as bilateral (Püschel et al. 2018) or unilateral bites (Ledogar et al. 2016), whereas the group with extrinsic loads can be used to model axial twist, lateral shake, pullback, and dorsoventral movements (Attard et al. 2014).

The values of the forces in the different scenarios can be obtained from different information sources (e.g., literature, experiments, other modeling approaches such as MDA, etc.) or can be arbitrarily selected. When comparing different extrinsic models, arbitrary values can be a good choice (Attard et al. 2014), whereas for the intrinsic cases the values of the muscular forces can be calculated as a muscular contraction (see muscular forces in the intrinsic cases).

Several authors have used multibody dynamic analysis (MDA) to previously predict bite forces or muscular forces as a source of information for the forces applied at the FEA models (Lautenschlager et al. 2018). A multibody dynamic system consists of solid bodies that are connected to each other by joints that restrict their relative motion. This kind of studies analyzes how mechanical systems move under the influence of forces and can also be used to identify which forces are produced during the dynamic behavior of the system under analysis. This topic is, however, out of the scope of this chapter and further exposition can be found in Curtis (2011) where the application of MDA in vertebrates is reviewed.

Muscular forces in the intrinsic cases. The external loads that are acting on a body are applied as force or pressure on a surface. In a dynamic analysis, muscles are acting in combination to create a succession of individual static cases with several component contributions through time. In a static analysis (which is the one we are mostly referring to here) the muscle can be simplified as a force vector with an associated value for a specific case study. It is usual to analyze the so-called "theoretical maximum" which is when all muscles are acting together in a maximal tetanic contraction.

Muscle forces are calculated using muscular cross-sectional areas and a value for the specific muscular tension of 0.3 MPa (force per unit area), which is assumed as muscular contraction. This value, estimated by Alexander (1992), is considered as an isometric contraction of each adductor muscle. The physiological cross-sectional area (PCSA) is the area of the cross-section of a muscle perpendicular to its fibers, generally at its widest point.

$$F = P \cdot A_{PCSA} \qquad \text{(equation 10)}$$

Where F is the muscle force, P is the specific muscular tension and A_{PCSA} is the physiological cross-sectional area.

Usually, when solving models of mammalian mandibles, the muscle forces (pterygoid, masseter, and temporalis) correspond to input values that have previously been calculated, whilst bite force is the output value solved by the static equations.

Muscular forces can be applied homogeneously on the insertion areas (Püschel et al. 2018) or can be distributed tangentially over the attachment areas wrapped around the bone surface (Tseng et al. 2017). To define the direction of the muscular forces, there are several accurate methods that create frames of linear elements all over the muscle attachments that linked the upper and lower jaws, with forces applied at the center of the frame (Attard et al. 2014). The simplest approach to determine the directions of the forces is defining the lines joining the centroid of the insertion area on the skull with the centroid of the insertion areas on the mandible (Panagiotopoulou et al. 2017, Püschel et al. 2018). In fact, if we assume homogeneous muscle force all over the muscle insertion, a single equivalent load applied at the centroid of the surface can replace a homogeneously distributed load applied on a surface. However, it should be mentioned that this single equivalent force generates little difference in the output values of stress and strain in the regions immediately outside of the applied force. This is because the specific force may create an artificially high stress (for more details see the problem of the maximum peak value addressed below).

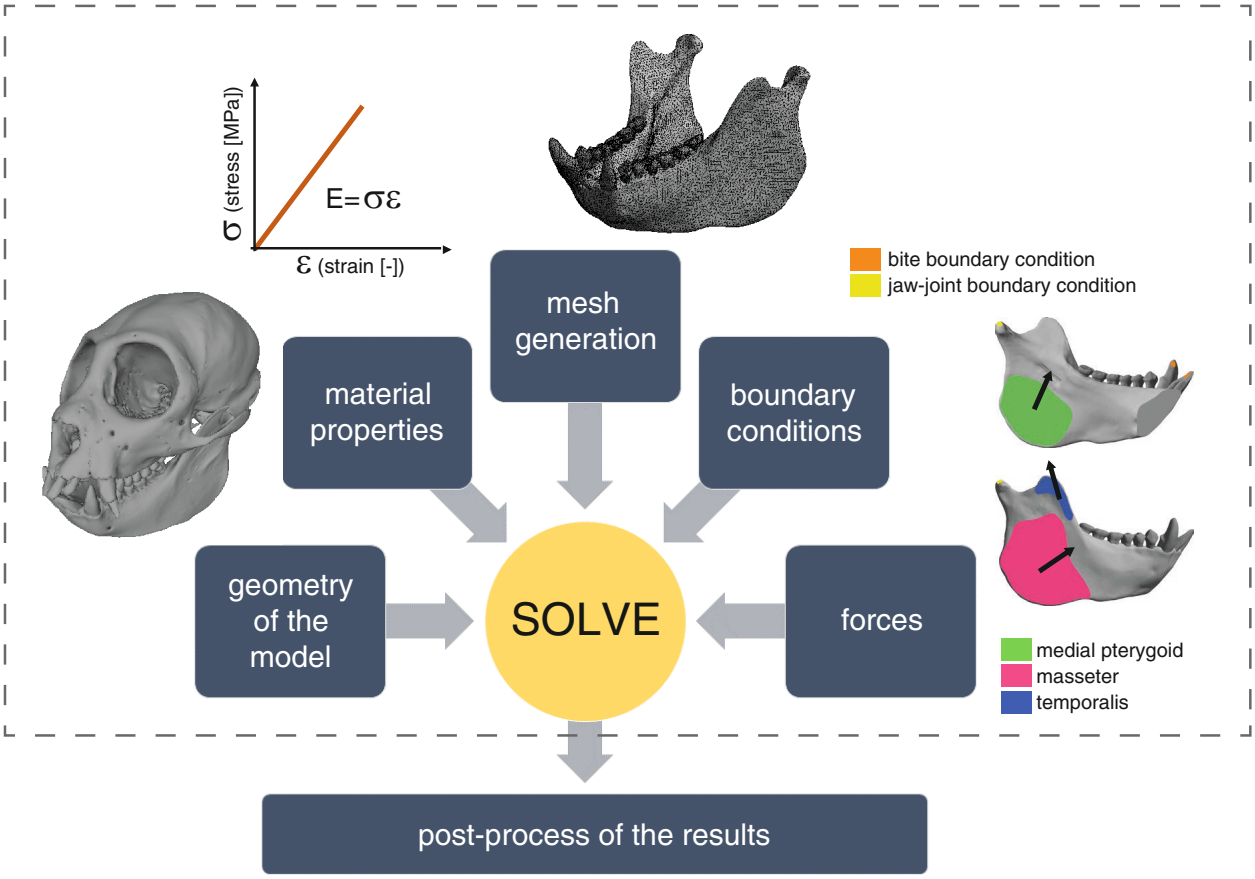

Fig. 4.5. Flow chart of a finite element analysis. All the steps involved in the post-process: Creation of the model's geometry, definition of the material properties, generation of the FEA mesh, definition of the boundary conditions and application of the forces.

Boundary conditions. Boundary conditions are defined to represent the unknown loads (for Newton's third law), displacements, and constraining anchors that the structure experiences during the action of the forces. In general, it is recommended to avoid over-constrained models and redundant supports. Redundant supports are those in excess when the equilibrium is already guaranteed. It means that the number of unknown loads is higher than the number of degrees of freedom of the body. In a FEA planar model, the degrees of freedom of the body are three (the displacements in both directions and the rotation on the plane). For example, in Marcé-Nogué et al. (2017b) the boundary conditions are fixing both directions in the jaw-joint and only the vertical displacement at the bite point. This is a total of three constraints which is exactly the number of degrees of freedom for a planar model. The degrees of freedom of the body are six when analyzing 3D models using solid elements: three displacements in each direction, and three rotations in each axis. Excessive constraints tend to add stiffness to the model, thus making it stiffer than it should be.

In addition, it is fundamental to avoid under-constrained models which could produce rigid-body motions of the model. This means that the number of unknowns is lower than the number of degrees of freedom and that we need to be sure that the model is fixed to avoid any possibility of translation or rotation.

In the case of mandibular models, boundary conditions are often defined so they represent the fixed displacements that mandibles experience during biting scenarios. The first boundary condition restrains the condyle at the level of the contact points with the mandibular fossa of the cranium. in order to represent the immobilization of the mandible, thereby constraining the translation of the jaw in all the directions.

In intrinsic cases, a second boundary condition is applied to individual dental positions by fixing the displacement in the vertical axis. They are usually applied at different dental positions in order to simulate different biting scenarios (e.g., molar or incisive bite). According to Newton's third law, the corresponding reaction force represents the unknown bite force.

When a unilateral bite is modelled, then the phenomenon of torsion has great importance because only one bite point is being considered on one side of the mandible (namely the working side), which means that there is a balancing side that is not directly acting in the biting action. In the balancing side, muscle forces can be reduced in order to remove a distractive tensile reaction force at the working side jaw to avoid being pulled apart (Greaves 1978, Spencer 1999).

In extrinsic cases, the fixed condition of the teeth is not used because instead of defining muscular forces to the posterior part of the mandible, a force is applied at the dental position. For cases in which the weight of the head and prey/food are simulated, this fixed condition of the teeth is also not considered because the weight of the prey/food is also applied to the teeth as a force.

Mesh generation. The mesh of a FEA model is a collection of interconnected elements joined at nodes, which defines the shape of the model where the physical problem will be solved using the mathematical equations of the FEM. Elements usually consist of triangles, quadrilaterals, tetrahedrals, hexahedrals or other simple convex polygons which simplify and discretize the geometry of the original model.

A problem can be solved as a two-dimensional model or as a three-dimensional model. However, different finite elements are required (see Marcé-Nogué et al. 2015 for further details about FEA meshes). When the geometry that is required to be meshed consists of surfaces or lines, it is necessary to use shell or beam elements projected in a three-dimensional space. These elements require different formulation compared to the standard solid elements used in three-dimensional models but, usually, FEM packages allow their easy implementation. Two-dimensional problems are solved using the equations of plane elasticity and the model can be meshed with planar elements, which means that it is required to consider their thickness.

Currently, the main commercial FEA packages include several methods to automatically generate the mesh of the desired geometry without human intervention. This improves the analysis, but the mathematical complexity of the FEM still means that mesh generation has to be treated with care. It is important to find a reasonable balance between the best mesh to be built and analyzed, and computational limitations. Depending on the specific package, software or the file format of the imported geometry, there are differences in the order of steps required to carry out a FEA. In some cases the mesh is generated in the first steps and then, the creation of the boundary conditions and the application of the forces are performed on the mesh (Figueirido et al. 2018) or, inversely, in other cases the inclusion of the forces and boundary conditions are performed on the geometry to then finally mesh the model (Püschel et al. 2018).

The different types of elements and the different types of mesh (structured, non-structured, uniform, non-uniform) and their pros and cons in the context of biological problems are discussed in detail in Marcé-Nogué et al. (2015). The quality assessment and the reliability of the mesh to solve FEA models is also discussed in Marcé-Nogué et al. (2015), and some examples of convergence results when the size of the elements is reduced can be found in Bright & Rayfield (2011b) and Tseng & Flynn (2015), where vertebrate species were analyzed.

Understanding the outputs of FEA

Scalar results. The solution of a FEA model generates several different outputs. A scalar is a quantity represented by a numerical value or magnitude that is independent of specific classes of coordinate systems, or one that is usually said to be described by a single real number. Strain energy or mechanical advantage are examples of scalar values. For example, they were used by Tseng et al. (2017) in FEA mandibular models to study the feeding capability in fossil and living Lutrinae. Based on their results, it was hypothesized that the extinct species of giant otter *Siamogale melilutra* exhibited feeding ecomorphological adaptations that have no living analog.

Vectorial results. FEA vectorial results are the ones represented by a vector. A vector is a quantity that has magnitude and direction and that is commonly represented by a directed line segment whose length represents the magnitude and whose orientation in space represents the direction. This can be also represented by separating the vector into two or three components depending on the dimensionality of the problem (i.e., 2D or 3D).

The force reactions derived by Newton's laws are vectorial results. In cranial mechanics, the bite force is computed as an output result when muscle forces are applied as input variables. Bite force strongly depends on the size (Wroe et al. 2005) of the models and needs to be carefully used when comparing models of dissimilar sizes. However, if analyzed properly, it can be used in a comparative setting to evaluate bite performances given different tooth positions (Figueirido et al. 2014).

Displacements are also a vectorial result providing the information from the original position of a node of the model with respect to the new position of the same node after being loaded by the input forces. These results have been used to compare the deformation between the unloaded and the loaded model (Gröning et al. 2011a).

Tensorial results. Tensors are important in physics because they provide a concise mathematical framework to formulate and solve problems of physics in areas such as stress, elasticity, fluid mechanics, and general relativity.

Stresses and strains are tensorial which means that they are represented by a tensor. Tensors are geometric objects that describe linear relations between geometric vectors, scalars, and other tensors and are represented by an organized multidimensional array of numerical values. The order (also known as degree or rank) of a tensor is the dimensionality of the array needed to represent it, or in other words, the number of indices needed to label a component of that array. For example, stresses and strains in three-dimensional models are represented by a matrix (a three-dimensional array) in a basis, and consequently correspond to a 3rd-order tensor.

In plane elasticity, tensors are kept as a third order tensor but with zero values in all the stresses related to the third direction in plane stress, and with zero values in all the strains related to the third direction in plane strain. Plane stress stays different from zero in ε_z and plane strain σ_z but these values are negligible with respect to the other values, and, therefore, we can assume plane elasticity as a two-dimensional solution and solve only the x-y components.

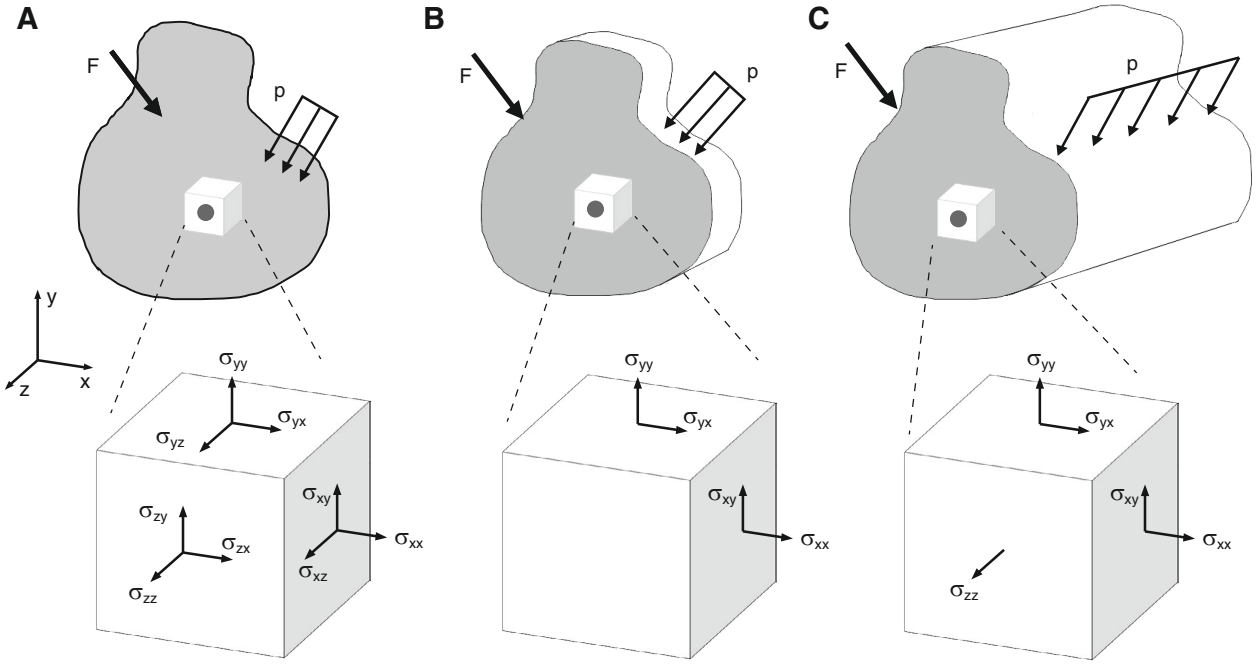

Fig. 4.6. Components of the tensor of stress in **A,** three-dimensions, **B,** plane stress and **C,** plane strain.

$$\sigma = \begin{bmatrix} \sigma_x & \sigma_{xy} & \sigma_{xz} \\ \sigma_{xy} & \sigma_y & \sigma_{yz} \\ \sigma_{xz} & \sigma_{yz} & \sigma_z \end{bmatrix} \quad \varepsilon = \begin{bmatrix} \varepsilon_x & \varepsilon_{xy} & \varepsilon_{xz} \\ \varepsilon_{xy} & \varepsilon_y & \varepsilon_{yz} \\ \varepsilon_{xz} & \varepsilon_{yz} & \varepsilon_z \end{bmatrix}$$

(equation 11 and 12, for three-dimension problems)

$$\sigma = \begin{bmatrix} \sigma_x & \sigma_{xy} & 0 \\ \sigma_{xy} & \sigma_y & 0 \\ 0 & 0 & 0 \end{bmatrix} \quad \varepsilon = \begin{bmatrix} \varepsilon_x & \varepsilon_{xy} & 0 \\ \varepsilon_{xy} & \varepsilon_y & 0 \\ 0 & 0 & \varepsilon_z \end{bmatrix}$$

(equation 13 and 14, for plane stress problems)

$$\sigma = \begin{bmatrix} \sigma_x & \sigma_{xy} & 0 \\ \sigma_{xy} & \sigma_y & 0 \\ 0 & 0 & \sigma_z \end{bmatrix} \quad \varepsilon = \begin{bmatrix} \varepsilon_x & \varepsilon_{xy} & 0 \\ \varepsilon_{xy} & \varepsilon_y & 0 \\ 0 & 0 & 0 \end{bmatrix}$$

(equation 15 and 16, for plane strain problems)

This means that, in order to define the stress state or the strain state of a FEA model, it is necessary to know all the values of the components of the respective tensors in each point of the model under analysis. FEA simplifies this statement by solving the stress and strain tensor in points inside each element of the mesh. It is important not to confuse the FEA elements with the sides of the square in Figure 4.6. The square in Figure 4.6 is not a FEA element but just the graphical representation of the Cartesian planes that are required to be known in a point when we want to know all the values of the stress/strain tensor.

Depending on the orientation of the plane under consideration, each component of the tensor represents a value of stress/strain: the component normal to the plane, called normal stress, and another component parallel to this plane, called the shearing stress. The symmetry of the stress/strain tensor simplifies the question to know only six values for defining all the tensor.

Principal and equivalent values. Principal stresses/strains are the maximum normal stress a body can have at a point of its body. It represents only normal stress and it does not have any shear stress component. Mathematically speaking, principal values are the ones in the tensor when the shear components are null. They are useful to summarize all the stress states of a FEA model for the two maximum and minimum values instead of using all the different values of the stress tensor.

$$\sigma = \begin{bmatrix} \sigma_I & 0 & 0 \\ 0 & \sigma_{II} & 0 \\ 0 & 0 & \sigma_{III} \end{bmatrix} \quad \varepsilon = \begin{bmatrix} \varepsilon_I & 0 & 0 \\ 0 & \varepsilon_{II} & 0 \\ 0 & 0 & \varepsilon_{III} \end{bmatrix}$$

Equivalent values are scalar values of stress that can be computed from the stress/strain tensor in order to summarize the stress state defined by all the components of the tensor to a unique value. In other words, an equivalent stress is the value of stress that creates a uniaxial stress state in the point to study, equivalent to the previous multiaxial stress state. The von Mises stress criterion, the Tresca criterion or the Rankine theory are different ways to reduce the multiaxial stress state to an equivalent stress. Von Mises and Tresca criteria are applicable for ductile materials whereas Rankine's theory is preferred for brittle materials (Chen & Saleeb 1994).

The von Mises criterion is the most popular criterion for predicting the yield of ductile materials. Bone can be assumed to be either brittle (Doblaré et al. 2004) or ductile (Dumont et al. 2009). However, according to Doblaré et al. (2004), when isotropic material properties are used in cortical bone, von Mises is the most accurate criterion for predicting fracture location. This probably explains why it is in fact the most common criterion used in mandibular mechanics (Panagiotopoulou et al. 2017, Piras et al. 2013, Püschel et al. 2018, Tseng et al. 2017).

Uses of stress and strain. There are several different approaches that have been applied to analyze the results derived from mandibular mechanics. While some works analyze stress (Attard et al. 2014, Lautenschlager et al. 2016, Püschel & Sellers 2016, Tseng et al. 2017), other focus on strain (Gröning et al. 2013, Oldfield et al. 2012,

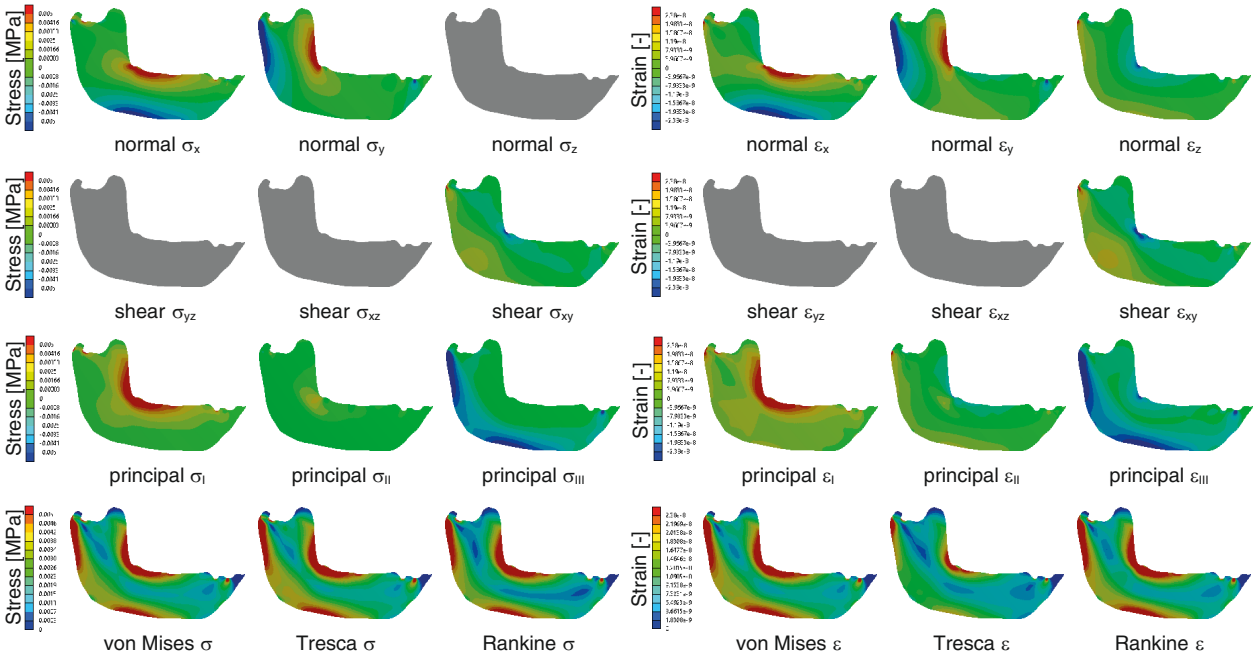

Fig. 4.7. Stress and strain distribution in a plane stress model. Considered are all the stress variables of the tensor, principal stresses and equivalent von Mises, Tresca and Rankine. Model of *Macaca fascicularis* from Marcé-Nogué et al. (2017b).

Panagiotopoulou et al. 2017). When using linear and elastic properties, it has been shown that both values are proportional and that the results of the distributions along the mandible are the same. This is due to the application of Hooke's law, which establishes a proportional relation between stress and strain.

Both stress and strain are accepted when comparing models below the fracture point, but, when we want to extrapolate these models to study fracture mechanics, a new debate is triggered: Is it stress or strain that causes failure? Probably the longest standing issue regarding failure criteria is whether they should be expressed in terms of stresses or in strains.

In engineering, the most commonly used form is the von Mises criterion expressed in terms of stress. Other criteria that are used are the maximum shear stress criterion (Tresca), the maximum normal stress criterion (Rankine) or the maximum normal strain criterion (Rankine). Despite the von Mises stress being a stress-designed criterion based on the maximum distortion of the strain energy, the stress-strain relations for isotropy can be used to convert the von Mises criterion in terms of stresses into a metric expressed in terms of strains. This transformation can be easily done using a simple mathematical procedure, but this does not obliterate the incontrovertible assumption that considers that all criteria can be switched from stress to strain (and vice versa). This is not always possible, especially when considering anisotropic material properties, but equally so for some isotropic cases. As an example, the maximum normal stress criterion and the maximum normal strain criterion take different forms when interconverted.

In this text, stress is taken as the fundamental form to be used when focusing on failure criteria. This is the direct consequence of the following conditions. Stress must be used if one wishes to have compatibility with fracture mechanics in the brittle range and with dislocation dynamics in the ductile range. Both of these classical theories require formulations in terms of stress.

On the other hand, strain has been shown valuable when comparing simulation results with experimental data (Bright & Rayfield 2011a, Gröning et al. 2012a), since strain gauges are commonly used in experimental settings. These electrical components experience changes in length as changes in resistance, and this property can be used to measure strain on a surface (e.g. bone) and compare it with FEA models.

Comparative framework

One of the most important decisions when comparing different specimens is the selection of taxa, provided that it allows to create an appropriate biological comparative framework. In addition, it is also important to build the models considering that they will be compared under equivalent loads in order to interpret the stress pattern differences of the models as a sign of relative strength. Comparing the strength allows to discern that more robust or stronger mandibles are needed to be able to process more demanding diets such as, for example, nuts, shells, or bones. A comparative framework can be defined as all the decisions we need to take into account in the post-processing of FEA models that enable the comparison between models to analyze the biomechanical behavior of different species or specimens under equivalent mechanical scenarios. Post-processing involves all the steps carried out after solving the FEA models. All these considerations are not necessary, if the purpose is to simply analyze the distribution of stress or strain of just one mandible, e.g. to compare it against real data or to study mandibular facture.

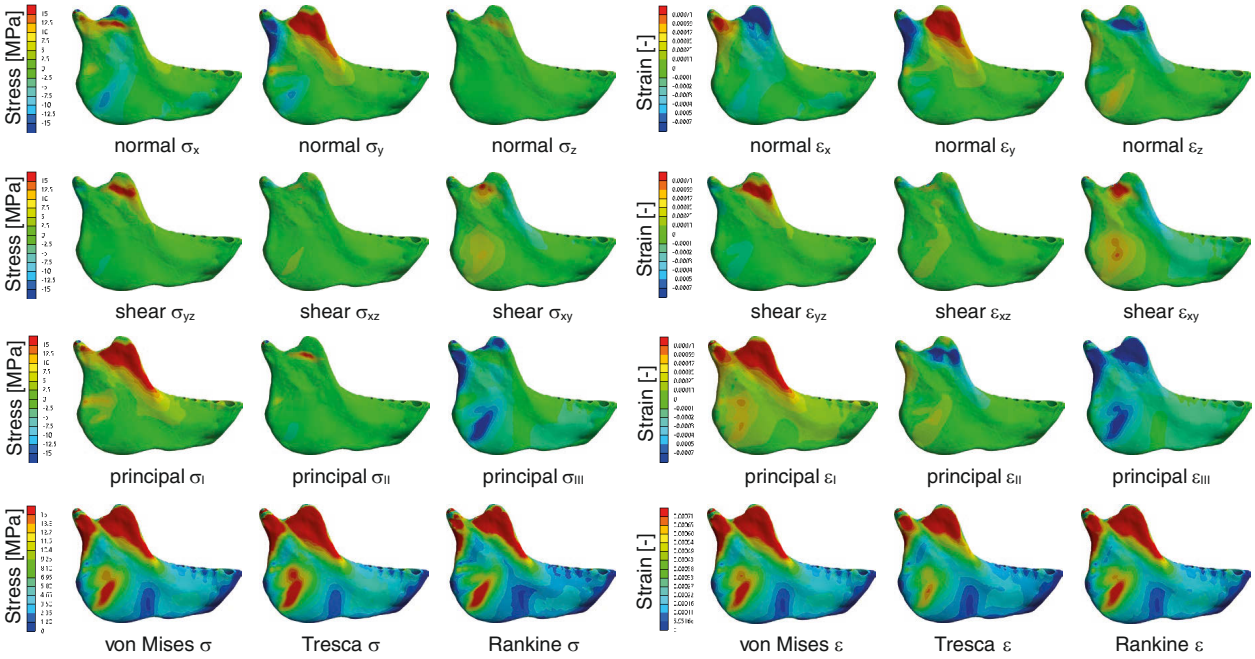

Fig. 4.8. Stress and strain distribution in a three-dimensional solid model. Considered are all the stress variables of the tensor, principal stresses and equivalent von Mises, Tresca and Rankine. Model of *Pithecia monachus* from Püschel et al. (2018).

Orientation of the models. All models must be oriented in the same way. Several options exist for mammalian mandibles, such as positioning them in an anatomical orientation, central occlusion or according to anatomical planes, such as the Frankfurt horizontal plane (Marcé-Nogué et al. 2017b, Osborn 1987). Another option is to apply algorithms such as a best-fit alignment to orient all the models with respect to a common plane (e.g., Püschel et al. 2018 applied to talar morphology). It is important to orient all models consistently because different orientations can result in different muscle force orientations, which can potentially have a significant effect in the variation of the results (Gröning et al. 2012b).

Scaling the models. When the analyzed specimens exhibit significant size differences, it is necessary to adjust the models to a comparable size. There are two main ways of answering the question of how performance can be compared so that the effects of size and shape are disentangled, in order to exclusively focus on how shape affects mechanical performance for a given loading condition (Dumont et al. 2009).

(1) Change the size of all the models to the same size and apply the same force.
(2) Keep the differences in size in the models and apply an appropriate force that generates the same effect as carrying out the procedure described in 1.

In vertebrate models, it is more common to follow the second approach, thus keeping the original size of the model. However, even though both approaches are correct, they display the results in a different context. Some recent works have discussed which equations should be used to scale the models to the same size in order to study the stress patterns or the strain energy (Dumont et al. 2009, Marcé-Nogué et al. 2013), thus proposing that size could be removed either by modifying the dimensions of the model, or the values of the muscular forces or muscular pressures applied. It is important to note that when comparing stress/strain the forces should be scaled in a different way than when comparing other values, such as displacements.

For FEA planar models, the forces applied should be scaled using – for example – the quasi-homothetic transformation proposed by Marcé-Nogué et al. (2013) to allow meaningful comparison between planar models. In this case, it is important to bear in mind if our planar models are following the equations of plane stress or plain strain. For FEA models in three-dimensions, the volume ratio should be considered for calculating the different forces. The equations that must be fulfilled between two models that are to be compared without the effect of size are shown in Table 4.4 depending on the elasticity problem used.

Some criticisms and improvements have been made in recent papers (Parr et al. 2012) regarding the widely used scaling methodology proposed by Dumont et al. (2009). In particular, the analysis of 3D complex biological structures

Table 4.4. Force equations in a scaled model B with reference to model A. A_A is the area of the reference model, A_B the area of the scaled model, t_A the thickness of the reference model, t_B the thickness of the scaled model, V_A the volume of the reference model and V_B the volume of the scaled model.

Model type	Comparing strain/stress	Comparing displacements
Plane stress	$F_B = \left(\sqrt{\frac{A_B}{A_A}}\right)\left(\frac{t_B}{t_A}\right) F_A$	$F_B = \left(\frac{t_B}{t_A}\right) F_A$
Plane strain	$F_B = \left(\sqrt{\frac{A_B}{A_A}}\right) F_A$	$F_B = F_A$
3D models	$F_B = \left(\sqrt[3]{\frac{V_B}{V_A}}\right)^2 F_A$	$F_B = \left(\sqrt[3]{\frac{V_B}{V_A}}\right) F_A$

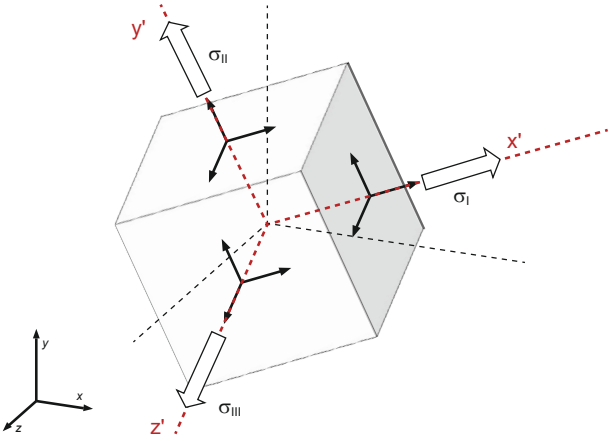

Fig. 4.9. Principal components of stress and principal directions.

has been improved, by considering complex inner cavities such as those present in skulls. In the latest literature it is possible to find several works focused on mammalian mandibles which followed the suggestions of Dumont et al. (2009) to scale their models in order to be able to compare von Mises stress via the surface ratio (e.g., Lautenschlager et al. 2016). Many other works have scaled their models using the volume ratio to then compare stress based on the allometric proportions between muscular forces and body mass (e.g. Attard et al. 2014, Tseng et al. 2017).

The main controversy regarding the scaling procedures is whether the scaling should be carried out by means of a surface ratio or via a volume ratio. Interestingly, authors such as Dumont et al. (2009) which propose the use of surface ratios, do not deny the usefulness of volume ratios when scaling models to compare von Mises stress. In fact, they define an "area proportion" which can be calculated from the areas but can also be deduced from volumes $[volume]^{2/3}$ or length $[length]^2$ which can be substituted for an area ratio. This means that both the surface ratio and the volume ratio are equivalent when the latter is raised to the ⅔ power. However, exchanging ratios in the equations cannot be done when comparing models that differ in shape, because models with different shapes do not necessarily have the same surface area to volume ratios.

To clarify some of the issues in this debate (i.e., how the scaling should be done when comparing von Mises stress), Marcé-Nogué et al. (2013) published a methodological paper that was later followed by a practical application for 3D models by Fortuny et al. (2015), where it was shown that the relationship using the equations of continuum mechanics should be made by means of the volume ratios and not using surface ratios. These results agree with the fact that muscular forces and body mass/volume are related with the ⅔ power (Meers 2003, Wroe et al. 2005).

Material properties. The difficulty of obtaining information on the material properties (namely Young's modulus and Poisson's coefficient) of bony structures due to the absence of data for the species under study or any close relatives, makes it very difficult to create a comparative framework with different material properties for each model. It is common to consider bone as an isotropic material for simulations, as real data for bone materials are unavailable for most species. Moreover, if the comparison is made between the same bony structures in close relatives, it makes sense to use the same material properties for all the specimens compared. This is the usual procedure when comparing mammalian mandibles (e.g., Serrano-Fochs et al. 2015, Tseng & Binder 2010), even though some authors have obtained heterogenic and orthotropic properties by carrying out experiments (Panagiotopoulou et al. 2017).

When linear and elastic material properties are assumed in a comparative analysis, the effect of the elastic modulus of the material is irrelevant for stress patterns. In the case of the strains and displacements, there is an inverse proportionality that is kept constant, between the values of the metrics and the changes in the elastic modulus. These properties allow comparative studies without considering the real elastic materials properties (Gil et al. 2015).

This evidence suggests that the use of the values that define a linear material (namely Young's modulus and coefficient of Poisson) is not crucial for the development of the analyses proposed here, because these values do not affect the results when a relative comparison of stress results between models is performed. In that sense, material properties should not be an issue when comparing bony structures.

Simplifications. Apart from the material properties discussed above, models are, by definition, a simplification of reality which means that one has to be aware of which assumptions are required, so as to keep them in mind when interpreting the results. There are at least two issues of great importance that should be considered in relation to model simplifications (when required):

(1) Knowing whether the model simplifications are not extremely affecting the sensitivity of the results.
(2) Carrying out the same simplifications in all the models under comparison in order to avoid non-comparable scenarios/results.

In that context, a sensitivity analysis will test the influence of the different parameters of the FEA models. For example, Gröning et al. (2012b) tested the sensitivity of FEA models of a human mandible with different trabecular bone defined as a solid inner material with a lower Young's modulus. For instance, this kind of analysis can give us information of how we can simplify trabecular bone without excessively changing the results of our models. Simplified modelling assumptions of material properties and muscle activation patterns may introduce analytical errors in analyses where quantitative accuracy is critical for obtaining rigorous results (Panagiotopoulou et al. 2017). For example, when comparing mammalian mandibles it is common to segment the models as solid models without including trabecular bone properties, since it has been shown that the exclusion of trabecular bone does not affect the general results of a comparative FEA (Fitton et al. 2015) and because it has been argued that simplified models can reproduce the overall stress distribution patterns in ex vivo validation experiments (Bright & Rayfield 2011a).

Additionally, it is common not to segment the periodontal ligament (PDL) despite some debate in the literature regarding the importance (or lack of it) of modelling this

tissue in models of the mandible in FEA (Bright 2014). Some modelling studies of the primate mandible have suggested that the presence or absence of the PDL might affect the obtained results substantially throughout the whole structure (Gröning et al. 2011a, Marinescu et al. 2005).

Another discussed simplification in mammalian mandibles is the accuracy of the results when analyzing planar models instead of 3D models. Planar models can be useful to get insights of the main patterns of variation of stress from both a morphological and a biomechanical perspective, as it has been exemplified by Fletcher et al. (2010), Marcé-Nogué et al. (2017b), Neenan et al. (2014), Piras et al. (2013), and Serrano-Fochs et al. (2015). Planar models can be consistent with the results obtained from more complex scenarios, even though the level of detail is not the same. Probably the most important reason is that planar models study a specific biological scenario that can be simplified, and the validity of the models will be accepted if they can achieve the objective for which they were created. For example, planar models of primate mandibles can be good FEA models when distinguishing hard and soft-food eaters because the use of this simpler models allows to distinguish these categories in terms of stress values (Marcé-Nogué et al. 2017b).

Planar models are easier and faster to build than 3D models and can also be a better option in some cases, as they allow the creation of models that would not be easy to carry out in 3D when the original data are impossible to reconstruct. On one side, in the field of paleontology it is usual to rely on morphotaxa defined from scarce and fragmentary elements of few individuals, which means that it could be potentially difficult to carry out reconstructions in three dimensions, but not equally so in two dimensions. On the other side, 3D reconstructions of the fossils can be difficult to produce if no access is granted to digitize the original materials.

Using FEA of mandibles to understand diet

The use of FEA to study the mechanics of mandibles and relating it to diet has been widely used in the last years (Fletcher et al. 2010, Gill et al. 2014, Gröning et al. 2011b, Lautenschlager et al. 2018, Marcé-Nogué et al. 2017b, Neenan et al. 2014, Piras et al. 2013, Püschel et al. 2018, Serrano-Fochs et al. 2015, Tseng & Binder 2010, Zhou et al. 2019). The underlying hypothesis is that under equivalent loads, the stress patterns observed in the different FEA models can be interpreted as a sign of the relative strength, with specimens with higher stress being weaker. Therefore, the hypothesis assumes that more robust or stronger mandibles would be needed to process more demanding diets. The study of extant species has been fundamental to this approach, because the information of the dietary preferences of extant species is readily available hence facilitating the correlation of this information with the results obtained using FEA models. Some examples are presented here, showing how authors have used FEA to infer or study the dietary preferences of different mammals.

Figueirido et al. (2014) exclusively analyzed extant species when comparing the results obtained in both cranial and mandibular FEA models of red and giant pandas, with the dietary differences of each one of these species reflecting their distinct bamboo feeding preferences. Püschel et al. (2018) studied the sclerocarpy adaptations in the mandible of pitheciid primates. This was done using FEA models which demonstrated that there is indeed a relative robusticity continuum for some aspects of shape, but this gradient could be related to other factors rather than sclerocarpic specialization. Finally, Marcé-Nogué et al. (2017b) studied a large number of planar models of different primate mandibles under different loading scenarios. They found that there are significant differences in mandibular biomechanical performance depending on food categories and/or food hardness in Primates.

The understanding of dietary preferences in extant species enables a comparative framework with fossil taxa to infer dietary preferences in extinct species. This is, probably, one of the most widely applied aspects of FEA for mandible biomechanics, both using three-dimensional and planar models.

In that sense, using planar models Fletcher et al. (2010) tested, if mandibles of hindgut-fermenter ungulates are more robust than those of ruminants. They addressed the question, if extinct hindgut or foregut fermenters can be identified in the fossil record. Similarly, Serrano-Fochs et al. (2015) studied FEA mandible models of armadillos. The results of this FEA showed that omnivorous species have stronger mandibles than insectivorous species, and also that the studied fossil herbivore taxa possess very strong mandibles due to a great amount of oral processing.

Three-dimensional models of extant taxa have been used in several carnivores to study fossil species. For example, Tseng & Binder (2010) compared strain distributions during a biting scenario between two bone-cracking ecomorphologies that evolved convergently, *Crocuta crocuta* and *Canis lupus*, and the fossil *Dinocrocuta gigantea*. *Kolponomos* has been interpreted as an otter-like shell-crusher based on a similar dentition. Tseng et al. (2016) studied different feeding strategies of extant carnivores in different FEA models. They tested whether there was a convergent morphology in the Miocene *Kolponomos* and the Pleistocene sabre-tooth felid *Smilodon* by using their anterior mandibles as anchors. The same authors studied the feeding capability of the Mio-/Pliocene giant otter *Siamogale melilutra* using FEA models of the mandible of different living Lutrinae to infer that the mandibular strength in *S. melilutra* strikingly surpasses molluscivores such as the sea otter and the Cape clawless otter (Tseng et al. 2017).

In fact, the combination of both FEA models of the mandible and skull has been common in the study of fossil carnivores. Others such as Wroe et al. (2007) studied the extinct marsupial wolf *Thylacinus cynocephalus* and the placental grey wolf, which are commonly presented as an iconic example of convergence. In spite of this convergence, comparisons of stress distributions in the FEA models not only revealed considerable similarity, but also provided informative differences suggesting ecological overlap yet different prey strategies. They suggest that the grey wolf is better adapted to withstand the high extrinsic loads likely to accompany social hunting of relatively large prey. Other authors (Attard et al. 2011) studied the biomechanical performance of the skull and mandible of *T. cynocephalus* in relation to those of two extant marsupial carnivores with

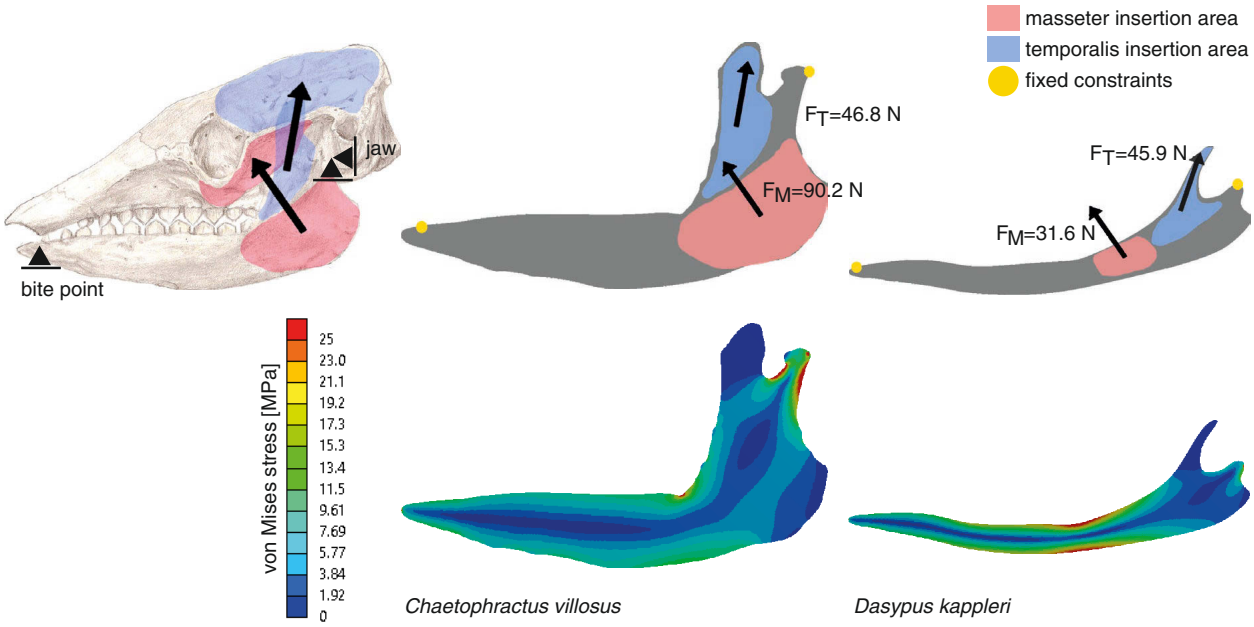

Fig. 4.10. Free-body and von Mises stress diagrams of armadillo mandibles with real muscular force values. **A,** free-body diagram of a mandibular bilateral bite using a plane stress approach and; **B,** von Mises stress from a finite element analysis of *Chaetophractus villosus* and *Dasypus kappleri* from Serrano-Fochs et al. (2015). Results using real muscular forces values.

known diets that occurred sympatrically – the Tasmanian devil, *Sarcophilus harrisii,* and the spotted-tailed quoll, *Dasyurus maculatus* – suggesting that *T. cynocephalus* is likely to have consumed smaller prey compared to its size. Oldfield et al. (2012) created several FEA models of ursids to predict the feeding behavior of the extinct *Agriotherium africanum*. According to these authors, the findings did not resolve whether the fossil was more likely a predator or a scavenger of large terrestrial vertebrates but showed that it was well adapted to resist the forces generated by either activity. Sabre-tooths have been examined by Wroe et al. (2013) using FEA models to suggest that, in many respects, the placental *Smilodon fatalis* was more similar to the marsupial *Thylacosmilus atrox* than to a conical-toothed cat. Similarly, Attard et al. (2014) used FEA models of marsupial carnivores to test whether the fossil species *Nimbacinus dicksoni* was more similar to its recently extinct relative *Thylacinus* or to several large living marsupials. This comparison in a key aspect such as feeding ecology suggested that it was a large-prey specialist.

The difficulties of comparing fossil taxa with extant species has driven a handful of works using FEA models of the mandible to study dietary preferences in extinct species only comparing them to their extinct close relatives. However, the advances in computational tools to perform virtual reconstruction and restoration techniques of the original morphology of fossils (Lautenschlager 2016) allow the creation of accurate and realistic three-dimensional models. In that line, Gill et al. (2014) studied the dietary specializations and diversity in feeding ecology of the earliest stem mammals using FEA. Three-dimensional models of the mandible of the early mammaliaforms *Morganucodon* and *Kuehneotherium* were analyzed suggesting that the lineage split during the earliest stages of mammalian evolution due to ecomorphological specialization and niche partitioning.

Table 4.5. Real muscular force values and obtained results: Bite force, mechanical advantage and strain energy of *Chaetophractus villosus* and *Dasypus kappleri* mandibles using a plane stress approach.

Taxon	Masseter force (N)	Temporalis force (N)	Bite force (N)	Mechanical advantage (MA)	Strain energy (mJ)
Dasypus kappleri	31.6	45.9	15.29	0.197	6.8667
Chaetophractus villosus	90.2	46.8	34.69	0.253	4.9075

Table 4.6. Scaled muscular force values and obtained results: Bite force, mechanical advantage and strain energy of *Chaetophractus villosus* and *Dasypus kappleri* mandibles using a plane stress approach.

Taxon	Thickness (mm)	Model area (mm^2)	Masseter force (N)	Temporalis force (N)	Bite force 1(N)	Mechanical advantage (MA)	Strain energy (mJ)
Dasypus kappleri	3.51	971.37	62.0	33.2	23.22	0.244	15.54
Chaetophractus villosus	4.94	1038.90	90.2	46.8	34.69	0.253	4.9075

Practical example B. Finite element analyses (FEA) were applied to assess the lower mandible biomechanics of *Dasypus kappleri* and *Chaetophractus villosus*. The free-body diagram of the mandible, including masseter and temporalis muscle forces, is the same as shown in previous examples (Fig. 4.10). Constraints are applied in the bite position and the jaw joint.

Reconstructed muscular force values: Firstly, we solve these FEA models using realistic values from muscular contraction in both models. The muscle forces are calculated, as explained previously, using the muscle insertion area and a value for the specific tension of 0.3 MPa (force per unit area) is assumed as muscular contraction.

Using FEA we can obtain the von Mises stress patterns of each mandible (Fig. 4.10) and the bite forces calculated by the software according to the equilibrium static laws (Tab. 4.5). As expected, the bite forces calculated here are almost identical to the ones calculated before using the equations of lever mechanics.

The von Mises stress distribution is similar for both mandibles, with lower stress magnitudes in the ramus, null values in the coronoid process, and higher values of stress in the corpus. The mandibular corpus of *D. kappleri* is narrower than the mandibular corpus of *C. villosus* which results in higher stresses appearing in the mandibular corpus of *D. kappleri* and shows that this mandible is at a higher risk of fracture during chewing. Moreover, *D. kappleri* spends more strain energy during the biting. If we consider the strain energy as a measure of structural stiffness, and higher energy meaning lower stiffness (Tseng et al. 2017), all these results are consistent with the ones from beam models also suggesting that *C. villosus* is capable to withstand higher bending moments than *D. kappleri* when chewing.

Summarizing, under the same conditions of chewing with the maximum isometric contraction of each muscle, *C. villosus* is capable of generating higher bite forces with lower stress values in the mandible. This is in line with the fact that *D. kappleri* is a generalist insectivore, whereas *C. villosus* consumes a more demanding omnivore diet.

Scaled muscle forces values: Secondly, we solve the same models by using the scaling approach for the values of the muscle forces. In order to compare the models, a scaling of the values of the forces is applied. We use the equations defined in Table 4.4, according to which we are comparing stresses in planar models using *Chaetophractus villosus* as the reference model (Tab. 4.6).

In this case, we assume both models have the exact same muscle forces applied but remove the effect of size. This is equivalent to the creation of two models with the same model area and the same values of forces. The results suggest a more fragile and weaker mandible for *D. kappleri* but the results are coherent with the same dietary conclusions.

New developments in the comparison of mammalian mandibles: the example of the armadillo mandible

Quantification of FEA results

In recent years, FEA models and the respective results have been compared in a predominantly qualitative way, by comparing the stress or strain distributions. Visual comparison using only the stress or strain distribution of contour plots can be a good option when the number of models to compare is small and the results are distinctive enough between the analyzed models. For example, in Tseng & Binder (2010), comparison of stress distributions during a biting scenario in *Crocuta crocuta*, *Canis lupus* and the fossil *Dinocrocuta gigantea* was feasible, because the differences in the graphical representation of the von Mises stress are clearly visible and distinct from one another. However, when the number of models to be compared increases, such comparison becomes difficult (Neenan et al. 2014) and more rigorous quantification of the FEA results is useful.

Quantifying stress data at specific points of a model has been useful in ecomorphological analyses (Attard et al. 2014, Fortuny et al. 2011, 2016, Piras et al. 2015, Serrano-Fochs et al. 2015), but to take into account the biomechanical behavior of the complete model, single mean values of stress were adopted as quantitative measurement to provide a metric of the relative strength of vertebrate structures. This approach involves computation of the von Mises stress averages in finite element models. In spite of this approach having been used in several paleobiological studies (Aquilina et al. 2013, Farke 2008, Figueirido et al. 2014, Fish & Stayton 2014, Neenan et al. 2014, Parr et al. 2012, Tseng 2009), we employed the recently proposed "weight-meshed values" and the "quasi-ideal meshes" to compute these values as adapted by Marcé-Nogué et al. (2016, 2017a). The latter is more robust, because it takes into account the effects caused by the different size of the individual mesh elements in a FEA model.

Similarly, the quantification and post-processing of the results of FEA models has also evolved to be combined with other morpho-functional methodologies such as geometric morphometrics (GM). FEA and GM outputs have been used in mandible models to explore questions in functional morphology, ecomorphology, macroevolution, among others, by applying standard statistical methods. These methods involve multivariate regressions, ANOVAs or PLSs (Maiorino et al. 2015, Piras et al. 2013) or, even, GM as a tool to analyze the deformations resulting from FEA analyses (Gröning et al. 2011a).

Finally, it is worth mentioning that the influence of the size of the individual elements of the FEA mesh in the results must be always taken into account by performing sensitivity analysis (Tseng & Flynn 2015). To avoid the influence of the size of the elements in the results, an 'intervals' method' was proposed by Marcé-Nogué et al. (2017a), which incorporates element volumes to provide an additional way of quantifying and comparing FEA results, thus avoiding the problems with the mesh. This method could allow for considerably more effective comparisons of finite element models, and maybe more precise distinction between dietary traits.

The problem of the maximum peak value

Maximum values of stress or strain (or peak stress/strain) could be potentially useful as a value to consider when comparing the biomechanical performance of different FEA models. However, peak stress and strain should not be taken into account because the value could be a numerical singularity, which is a well-known problem in FEA (Morris 2008).

This singularity could be a consequence of a boundary condition or a perfect square within the geometry. A simply supported condition is an idealistic assumption. This condition has been applied specially in planar models, as in the examples provided by this chapter, where fixed displacements were imposed at the bite position and at the jaw joint in a simple point of the model. This condition creates a numerical effect that leads to the stress increasing without limit when the mesh is refined for both 2D and 3D elements. In 3D models of mandibles, simply supported conditions are usually applied in the bite position or in the jaw joint where the displacements are restrained in a specific area of the model. In a similar way, the perfect square condition is also an idealistic assumption where a corner with zero radius in the original geometry creates a stress concentration that also leads the value to increase without limit when the mesh is refined. To avoid artificially high stress magnitudes, it is not recommended to record the maximum stress or strain values in the whole model, because maximum values could be the result of singular high yet unrealistic magnitudes. As some authors have warned (e.g., Rayfield 2007), it may be difficult to assess the peak stresses of the model in the whole model. Some approaches regarding how to handle this problem are described in Marcé-Nogué et al. (2015). For example, this can be achieved by just studying the results obtained from an area of the model that is far enough from the artificially high magnitudes, or by adapting the mesh to avoid the visualization of this high value. Coarse meshes can avoid these extremely high stress values whereas very fine meshes can concentrate these high values in a very small region of the model. Finally, other authors have suggested to exclude elements displaying the stress or strain values within the top 5 % (Tseng & Flynn 2018).

Use of specific points to quantify data

Quantifying stress or strain data at specific points has been useful in ecomorphological analyses of mammalian mandibles. An example of this can be found in Attard et al. (2014) who selected equidistant points along the mandible to measure the distribution of von Mises stress for each loading case and then compared them with other models. This approach allows us to plot these values of stress in a graph where one of the axes is the value of stress and the other one is the position from anterior to posterior along the mandible.

This approach has also been used in combination with the values of von Mises stress in specific points with data from morphometric analysis in other vertebrate groups (Fortuny et al. 2011). Or in a different way, using the values of stress from the specific points to plot in a dispersion plot of a principal component analysis (PCA) (Fortuny et al. 2016, Marcé-Nogué et al. 2015). Quantifying data from FEA models allows the use of such data to test the significance using statistics or other methods, opening the door to new methodologies to be used in combination of FEA.

Case example: armadillos

Biomechanical problem and FEA data. Finite element analyses were applied to assess the lower jaw biomechanics of cingulate xenarthrans in Serrano-Fochs et al. (2015). The main goal of this work was to make a comparative assessment of the biomechanical capabilities of the mandible based on FEA, and to relate the obtained stress patterns with dietary preferences. To do this, a comparative framework was created following the indications of the previous section of this chapter, so to solve the biomechanical problem described in the free-body diagram of Figure 4.11. The mandible was constrained at the most posterior part and at the condyle level of the mandibular notch following the procedures described in Serrano-Fochs et al. (2015) and Marcé-Nogué et al. (2016, 2017a).

Planar models of 11 armadillo mandibles (Tab. 4.1), each one corresponding to a different species, were created. Two main masticatory muscles (i.e., temporalis and masseter) were included in the model as a vector between the centroid of the muscular attachment on the mandible and the centroid of the equivalent muscle attachment on the skull. To compare the models, a scaling of the values of the forces was applied using the equations defined in Table 4.4 in order to compare stresses in planar models, by using *Chaetophractus villosus* as reference model (Tab. 4.7).

Isotropic and linear elastic properties were assumed for the bone. In the absence of data for Cingulata or any other closer relative, and due to the absence of data for any mammalian clade with a similarly shaped mandible, the authors decided to apply the mandibular material properties of *Macaca rhesus*: E (elasticity modulus) = 21000 MPa and v (Poisson coefficient) = 0.45 (Dechow & Hylander 2000). The available properties of *Macaca rhesus* were chosen, provided that it has a wide range of habitats and diet which resembles omnivorous or generalist insectivorous diets, as observed in the analyzed armadillos (Richard et al. 1989).

The stress distribution obtained in each armadillo is shown in Figure 4.12A. These stress patterns can be interpreted as a sign of relative strength. Assuming that more robust or stronger mandibles would be needed both for processing harder food items, insect-feeding armadillos (which have none or little processing in the mouth) should be expected to have weaker mandibles (i.e. with higher stress levels) than those feeding on other items, such as herbivorous or omnivorous species.

On the other hand, differences in stress distribution patterns may provide a clue regarding different aspects of the feeding ecology of the analyzed species. The aim of the methods presented below is to show that using a comparative framework and post-processing the results (e.g., with specific points, mesh-weighted values, quasi-ideal meshes or the intervals' method) the interpretation of the results can be greatly improved.

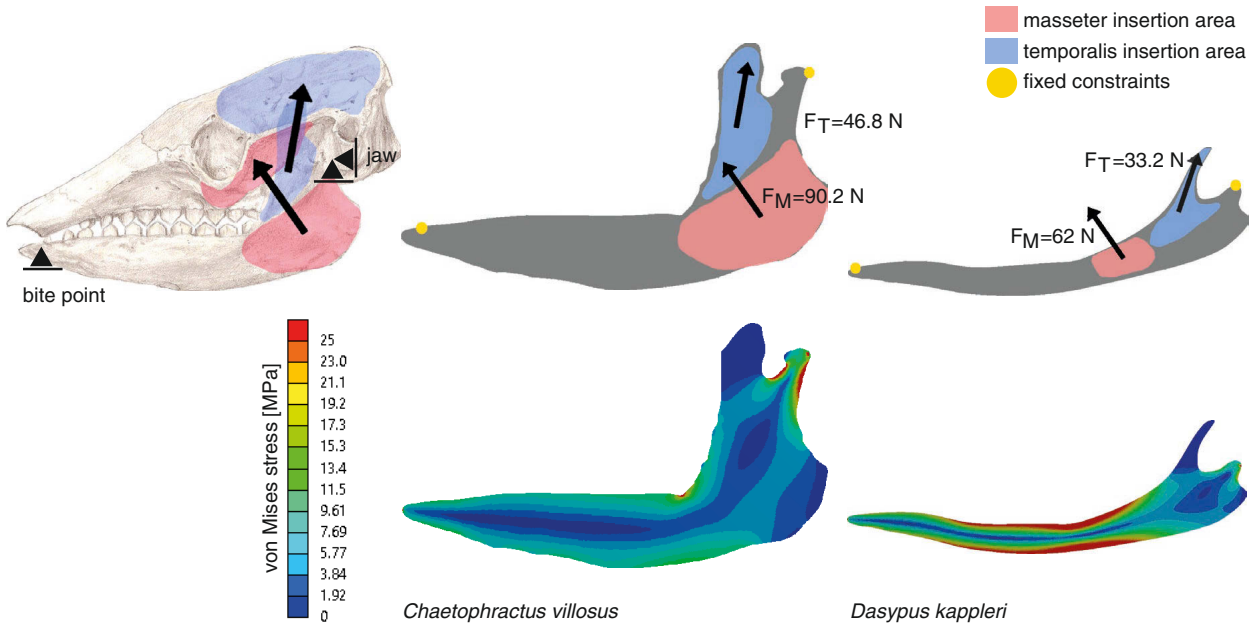

Fig. 4.11. Free-body and von Mises stress diagrams of armadillo mandibles with scaled muscular force values. **A,** Free-body diagram of a mandibular bilateral bite using a plane stress approach; **B,** von Mises stress from a finite element analysis of *Chaetophractus villosus* and *Dasypus kappleri* from Serrano-Fochs et al. (2015). Results using scaled muscular force values.

Specific points. In Serrano-Fochs et al. (2015) the strength of the mandibles was studied using the values of stress in eight specific points. The values of stress in each specific point were plotted according to the different dietary traits of the studied armadillos. They are classified as omnivores or insectivorous specialists and generalists (Fig. 4.12A) and a Kruskal-Wallis test was applied to check if there were significant differences in the results. However, despite the lack of significant results, some patterns appear in the boxplots for some specific points (Fig. 4.12B). Moreover, a principal component analysis (PCA) of the stress values for all specific points recorded was carried out using the variance-covariance matrix (Fig. 4.12C). The aim of these analyses was to evaluate the stress values in a multivariate manner and to look for diet-related patterns.

The most obvious result is that in general, insectivorous species showed a larger variance than omnivorous species, and also that omnivorous species have some coincident stress patterns. However, the absence of significant results could be due to a lack of statistical power, or possibly because the selected points represent local non-significant regions, or the specific points were hindered by the lack of information about the whole FEA model.

Mesh-weighted average values and quasi-ideal mesh. A quantitative single measurement of the relative strength of the studied structure could be preferred to summarize the strength of the whole model. The most common approach has been the computation of the average von Mises stresses of the various models considered. Even though

Table 4.7. List of the species analyzed in the present study. The classification of each species was made on the basis of the current knowledge about the ecology of armadillos (see Serrano-Fochs et al., 2015 for discussion). The geometric properties and the applied forces by the masseter and temporalis muscles are also provided. Abbreviations preceding the names of institutions are used to identify the location were the specimens are housed. AMNH, American Museum of Natural History, New York, USA; MNCN, Museo Nacional de Ciencias Naturales, Madrid, Spain; MNHN, Muséum national d'Histoire naturelle, Paris, France; ZMB, Museum für Naturkunde (Zoologisches Museum), Berlin, Germany; MLP, Museo de la Plata, La Plata, Argentina.

Taxon	Diet	Collection number	Thickness (mm)	Model area (mm^2)	Masseter area (mm^2)	Temporalis area (mm^2)	Masseter force (N)	Temporalis force (N)
Priodontes maximus	Specialist insectivore	AMNH 208104	6.41	2051.70	616.02	255.06	1.29	0.53
Cabassous unicinctus	Specialist insectivore	MNHN 1953/457	3.51	415.75	112.08	22.91	0.37	0.08
Tolypeutes matacus	Generalist insectivore	AMNH 246460	3.56	497.40	157.01	64116.00	0.35	0.14
Dasypus kappleri	Generalist insectivore	MNHN 1995/207	3.51	971.37	105.37	153.18	0.28	0.41
Dasypus sabanicola	Generalist insectivore	ZMB 85899	2.78	527.86	150.66	71545.00	0.27	0.13
Dasypus novemcinctus	Generalist insectivore	AMNH 133338	2.94	613.54	225.77	92174.00	0.32	0.13
Chlamyphorus truncatus	Generalist insectivore-fossorial	ZMB 4321	2.00	113.19	16035.00	34006.00	0.04	0.09
Chaetophractus villosus	Omnivore / Carnivore	MNCN 2538	4.94	1038.90	300.58	156.08	0.66	0.34
Chaetophractus vellerosus	Omnivore / Carnivore	MLP 18.XI.99.9	3.68	538.80	145.04	117.03	0.30	0.24
Euphractus sexcinctus	Omnivore / Carnivore	MNHN 1917/13	5.66	1019.20	331.22	190.60	0.72	0.41
Zaedyus pichiy	Omnivore / Carnivore	MLP 9.XII.2.10	3.51	327.35	89737.00	66091.00	0.23	0.17

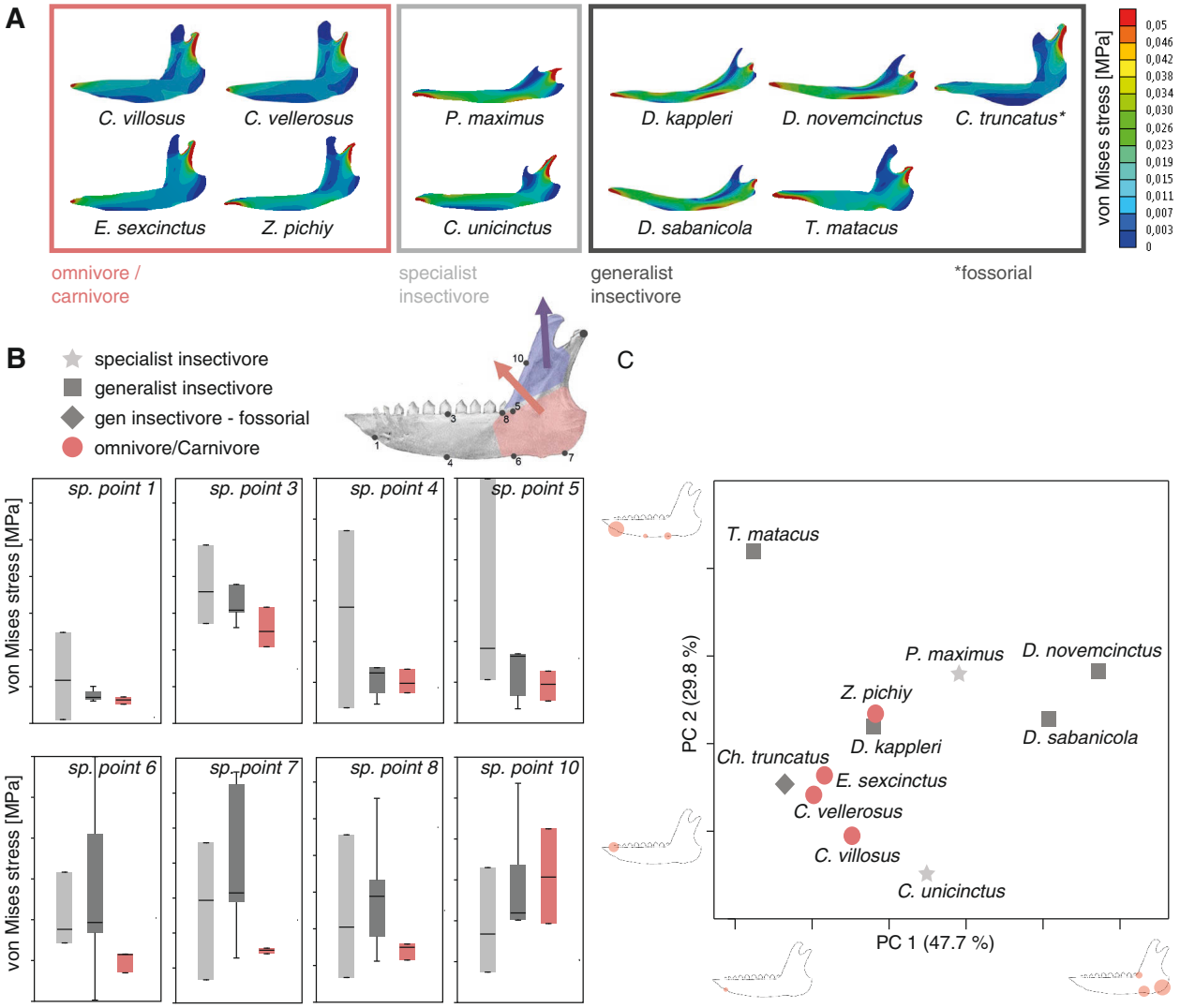

Fig. 4.12. Von Mises stress and PCA of armadillo mandibles according to diet. **A,** distribution of von Mises stress in the 11 armadillos' mandibles separated by diet: Omnivore/carnivore and specialist or generalist insectivore. **B,** boxplots of the von Mises stress values for the specific points; **C,** dispersion graph of the two first principal components. A hypothetical lower jaw is represented in each extreme of the axes, highlighting those landmarks with higher loadings in each PC (i.e., that have more importance in that PC) with red circles. The size of the circles approximates the standardized value of the loading. Modified from Serrano-Fochs et al. (2015). Abbreviations: *P. maximus*, *Priodontes maximus*; *C. unicinctus*, *Cabassous unicinctus*; *T. matacus*, *Tolypeutes matacus*; *D. kappleri*, *Dasypus kappleri*; *D. sabanicola*, *Dasypus sabanicola*; *D. novemcinctus*, *Dasypus novemcinctus*; *Ch. truncatus*, *Chlamyphorus truncatus*; *Ch. villosus*, *Chaetophractus villosus*; *Ch. vellerosus*, *Chaetophractus vellerosus*; *E. sexcinctus*, *Euphractus sexcinctus*; *Z. pichiy*, *Zaedyus pichiy*.

this approach has been used previously in paleobiological studies of mammalian mandibles (Figueirido et al. 2014, Neenan et al. 2014, Wroe et al. 2013), it represents a common error that should be avoided. When obtaining descriptive statistics from FE models, such as mean or median values, the problem of having non-uniform meshes is crucial and could lead to skewed results. For example, if by chance high stress values are obtained in larger elements, these high stress values will be under-represented because they are present in fewer elements despite the area with high values being large.

To solve this issue, Marcé-Nogué et al. (2016) proposed the so-called weight-meshed values, which take into account the type and size of the finite element mesh: mesh-weighted average mean (MWAM) and mesh-weighted median (MWM). In the same work, Marcé-Nogué et al. (2016) proposed the creation of quasi-ideal meshes (QIM) which are meshes where all the elements have practically the same size. The use of QIM avoids the use of weight-meshed corrections in the mesh, thus allowing the use of average values without correcting them. Moreover, with the use of QIM it is also proposed to use percentile values (e.g., 25th, 50th, 75th or 95th) as quantitative values, which allows to visualize the distribution of stress in each FEA model as a boxplot, facilitating the comparison between models. Moreover, and following the idea proposed by Walmsley et al. (2013), the use of the 95th percentile can be assumed as the maximum peak value to avoid the necessity to consider numerical singularities.

The arithmetic mean is calculated by summing all individual observations or items of a sample and dividing this sum by the number of items in the sample. In FEA results of stress, the arithmetic mean (AM) would be the sum of the value of the von Mises stress (σ_{VM}) of each element

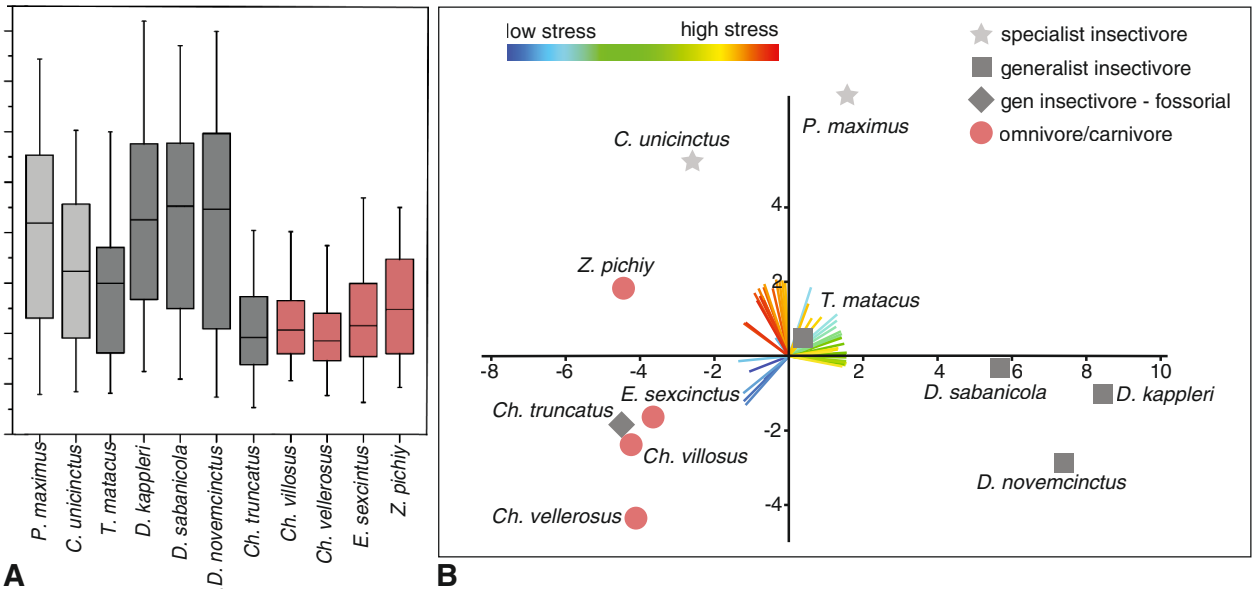

Fig. 4.13. Von Mises stress and PCA of armadillo mandibles under assumption of quasi-ideal meshes. **A,** boxplots of von Mises stress distributions when quasi-ideal meshes (QIM) are assumed for the Cingulata mandibles analyzed; **B,** PCA based on the correlation matrix. The loadings for each variable are colored according with the range of stress they represent, with reddish colors for high level of stress, and bluish for low levels. X-axis: PC1. Y-axis: PC2. Modified from Marcé-Nogué et al. (2016, 2017a). Abbreviations: *P. maximus*, *Priodontes maximus*; *C. unicinctus*, *Cabassous unicinctus*; *T. matacus*, *Tolypeutes matacus*; *D. kappleri*, *Dasypus kappleri*; *D. sabanicola*, *Dasypus sabanicola*; *D. novemcinctus*, *Dasypus novemcinctus*; *Ch. truncatus*, *Chlamyphorus truncatus*; *Ch. villosus*, *Chaetophractus villosus*; *Ch. vellerosus*, *Chaetophractus vellerosus*; *E. sexcinctus*, *Euphractus sexcinctus*; *Z. pichiy*, *Zaedyus pichiy*.

divided by the number of elements of the mesh (equation 19).

$$AM = \frac{\Sigma_{i=0}^{n} \sigma_{VM}}{n} \qquad \text{(equation 19)}$$

The mesh-weighted arithmetic mean (MWAM) corresponds to the sum of the value of the von Mises stress for each element multiplied by its own area (A) and divided by the total area (equation 20). This value is equivalent to the division of the arithmetic mean of the product of stress and area by the arithmetic mean of the area, which is easier to calculate and does not require correction of weight element by element.

$$MWAM = \frac{\Sigma_{i=0}^{n}(\sigma_{VM}^{i} \cdot A^{i})}{\Sigma_{i=0}^{n} A^{i}} = \frac{\frac{\Sigma_{i=0}^{n}(\sigma_{VM}^{i} \cdot A^{i})}{n}}{\frac{\Sigma_{i=0}^{n} A^{i}}{n}} = \frac{AM(\sigma_{VM}^{i} \cdot A^{i})}{AM(A^{i})}$$

(equation 20)

The median is the middle measurement of any set of sorted data. In the case of FEA, the median would be the value separating the higher half from the lower half of the values of von Mises stress recorded in each element of the mesh after they have been ordered.

Here the mesh-weighted median (MWM) of stress distribution has been defined as the division of the median of the product of stress and area by the median of the area (equation 21), based on the formulation presented in equation 20.

$$MWM = \frac{median\,(\sigma_{VM}^{i} \cdot A^{i})}{median\,(A^{i})} \qquad \text{(equation 21)}$$

Two indicators were proposed to evaluate whether a mesh is uniform enough to use the raw stress data for statistical analysis: the percentage error of the arithmetic mean (PEofAM) and the percentage error of the median (PEofM). These two indicators evaluate the difference between the non-weighted value and the weighted value of mean and median (PEofAM in equation 22 and PEofM in equation 23),

$$PEofAM = \left(\frac{MWAM - AM}{MWAM}\right) \times 100 \qquad \text{(equation 22)}$$

$$PEofM = \left(\frac{MWM - M}{MWM}\right) \times 100 \qquad \text{(equation 23)}$$

If the mesh of the model is close to an ideal fine uniform mesh, the non-weighted and the weighted indicators should be equal. If the error is lower than a certain threshold, the mesh can be considered a QIM, and quantitative and statistical analysis of the FEA data can be computed without any corrections and e.g., the percentile values 25th, 50th, 75th and 95th can be computed.

When this approach was used to analyze the armadillo mandibles, the significant differences among different diets found in the statistical analyses were more conclusive than the results obtained when analyzing stress values at a few specific points (Serrano-Fochs et al. 2015). This supports the analysis of the stress values of the whole specimen rather than focusing on just a few isolated points. An alternative would be to use both sources of information as isolated points, which could give an alternative view of some specific areas.

Statistics showed significant results when comparing omnivore and insectivore species (Tab. 4.8). However, this significance should be interpreted as illustrative more

than fully conclusive. This is because when a Bonferroni correction was applied, the mean values between specialized insectivores and omnivores are non-significant (most probably due to the small sample size of the specialist insectivores).

Intervals' method. In Marcé-Nogué et al. (2017a), a new method was proposed, named the intervals' method, that can be used to analyze data from finite element models in a comparative multivariate framework. As a case study, several armadillo mandibles were analyzed with success, showing that the proposed method was useful to distinguish and characterize biomechanical differences related to diet/ecomorphology.

This so-called intervals' method consists of generating a set of variables, each one defined by an interval of stress values. Each variable is expressed as a percentage of the area (in planar models) or the volume (in 3D models) of the mandible occupied by those stress values. Once all the stress values of a single specimen are obtained, they can be subdivided into different intervals, each one of them representing the amount of area in percent values of the original model having a specific range of stress values.

Afterwards these newly generated variables can be analyzed using multivariate methods. The use of this new method in the FEA models of cingulate mandibles allowed us to positively discriminate between specialist and generalist species of insectivores, which was not possible with the approaches defined above. The method described in Marcé-Nogué et al. (2017a) requires the definition of certain parameters such as a fixed upper threshold (FT_{upper}) and a specific number of intervals N. For example, in this work, $FT_{upper} = 0.1$ MPa and $N = 50$. This value is assumed based on the convergence procedure defined in Marcé-Nogué et al. (2017a), when the results of the regressions of the PCs indicate that the scores are almost completely correlated.

We carried out a PCA using the variance-covariance matrix (Fig. 4.13). The PCA of the correlation matrix successfully distinguishes the main three diets, with omnivore-carnivore species on lower-left area of the plot. PC2 separates specialist insectivores from the rest of species, while *Chlamyphorus truncatus* (i.e., a generalist insectivorous species exhibiting a very particular diet due to its completely fossorial lifestyle) is located near the omnivore/carnivore species in the negative part of the PC1 and PC2. Within this PCA, omnivore/carnivore species were characterized by very low stress values (lower-left quadrant of the plot), whilst generalist insectivores showed a proportionally larger area of intermediate stress values than the rest of the species. Specialist insectivores have proportionally larger areas of high stress.

Further usage of quantification of stress

Once we have quantified our models using specific points, average values or percentiles from a QIM or applying the intervals' method, we can use different ideas and methods to organize our data. On one hand, values of specific points, scalar values from the models (such as strain energy) and the mesh-weighted proposed averages values can be used for the comparison of models and their behavior. On the other hand, the intervals' method or the use of the stress quartiles are a good approach to check similarities between models.

Scalar values from the FEA models such as the strain energy were used to compare with other scalar values such as the mechanical advantage (Tseng et al. 2016) or used in regression with other values such as the volume of the model to check for allometry (Tseng et al. 2017).

Average values were used to compare different dietary traits and hardness of ingesta in planar FEA models of extant primates (Marcé-Nogué et al. 2017b), showing that there is a strong association between mandibular biomechanical performance, mandibular form, food hardness, and diet categories. The same work (Marcé-Nogué et al. 2017b) used average values to estimate the ancestral states for internal nodes using maximum likelihood and then by interpolating the states along the branches of the phylogeny. This approach was applied to get insights about the possible evolution of mandibular stiffness.

Finally, it is worth mentioning that the use of the different percentile values as a unique set of multivariate data, the average values or the powerful intervals' method, are all opening a window of opportunity for post-processing FEA-derived data. Using these kinds of data allows the application of multivariate analysis, and they can even be used to run machine learning algorithms in order to infer dietary preferences of fossil taxa from the data of living species. Both supervised (Marcé-Nogué et al. 2020) and unsupervised (Zhou et al. 2019) algorithms can be used to study mandibular biomechanics and its relationship with diet.

Table 4.8. Statistics for the Kruskal-Wallis test: mesh-weighted arithmetic mean (MWAM), and mesh-weighted median (MWM).

		Pairwise test p-value: Bonferroni non-corrected/corrected		
	Kruskall-Wallis p-value	Specialist insectivore vs. generalist insectivore	Specialist insectivore vs. omnivore	Generalist insectivore vs. omnivore
MWAM	0.0089	0.8197/1	0.0369/0.1107	0.0058/0.0173
MWM	0.0081	0.5676/1	0.0358/0.1073	0.0057/0.0170

Acknowledgments

The author was supported by the Deutsche Forschungsgemeinschaft (DFG, German Research Foundation, KA 1525/9-2). This research forms part of the DFG Research Unit 771 "Function and performance enhancement in the mammalian dentition – phylogenetic and ontogenetic impact on the masticatory apparatus." Thomas A. Püschel is acknowledged for his technical and scientific comments on earlier versions of this chapter and Dan Sykes for his help proof-reading this work. The author wants to thank the CERCA program (Generalitat de Catalunya) and Lluís Gil, Josep Fortuny and Soledad de Esteban-Trivigno for reading and commenting earlier versions of this work. Last but not least, the review comments by Stefan Lautenschlager and Jack Tseng greatly improved this chapter.

References

* indicates publications that originated from the DFG Research Unit 771.

Alexander, R. M. (1992): Exploring Biomechanics. Animals in Motion. New York Scientific American Library.

Alexander, R. M. (2005): Mechanics of animal movement. Current Biology 15: 616–619.

Aquilina, P., Chamoli, U., Parr, W. C. H., Clausen, P. D. & Wroe, S. (2013): Finite Element Analysis of three patterns of internal fixation of fractures of the mandibular condyle. British Journal of Oral and Maxillofacial Surgery 51: 326–331.

Attard, M. R. G., Chamoli, U., Ferrara, T. L., Rogers, T. L. & Wroe, S. (2011): Skull mechanics and implications for feeding behaviour in a large marsupial carnivore guild: The thylacine, Tasmanian devil and spotted-tailed quoll. Journal of Zoology 285: 292–300.

Attard, M. R. G., Parr, W. C. H., Wilson, L. A. B., Archer, M., Hand, S. J., Rogers, T. L. & Wroe, S. (2014): Virtual reconstruction and prey size preference in the mid Cenozoic thylacinid, *Nimbacinus dicksoni* (Thylacinidae, Marsupialia): PLoS One 9: e93088

Biknevicius, A. R. & Ruff, C. B. C. (1992): The structure of the mandibular corpus and its relationship to feeding behaviours in extant carnivorans. Journal of Zoology 228: 479–507.

Bouvier, M. (1986a): A biomechanical analysis of mandibular scaling in Old World monkeys. American Journal of Physical Anthropology 69: 473–482.

Bouvier, M. (1986b): Biomechanical scaling of mandibular dimensions in New World monkeys. International Journal of Primatology 7: 551–567.

Bright, J. A. (2014): A review of paleontological finite element models and their validity. Journal of Paleontology 88: 760–769.

Bright, J. A. & Rayfield, E. J. (2011a): Sensitivity and ex vivo validation of finite element models of the domestic pig cranium. Journal of Anatomy 219: 456–471.

Bright, J. A. & Rayfield, E. J. (2011b): The response of cranial biomechanical finite element models to variations in mesh density. Anatomical Record 294: 610–620.

Chen, W.-F. & Saleeb, A. F. (1994): Constitutive Equations for Engineering Materials: Elasticity and Modeling. Elsevier.

Christiansen, P. & Wroe, S. (2007): Bite forces and evolutionary adaptations to feeding ecology in carnivores. Ecology 88: 347–358.

Crompton, A. W. & Parkyn, D. G. (2009): On lower jaw of *Diarthrognathus* and the origin of the mammalian lower jaw. Proceedings of the Zoological Society of London 140: 697–749.

Cuff, A. R. & Rayfield, E. J. (2013): Feeding mechanics in spinosaurid theropods and extant crocodilians. PLoS One 8: e65295.

Cunningham, J. A., Rahman, I. A., Lautenschlager, S., Rayfield, E. J. & Donoghue, P. C. J. (2014): A virtual world of paleontology. Trends in Ecology and Evolution 29: 347–357.

Curtis, N. (2011): Craniofacial biomechanics: An overview of recent multibody modelling studies. Journal of Anatomy 218: 16–25.

de Esteban-Trivigno, S. (2011): Ecomorfología de xenartros extintos: Análisis de la mandíbula con métodos de morfometría geométrica. Ameghiniana 48: 381–398.

Dechow, P. C. & Hylander, W. L. (2000): Elastic properties and masticatory bone stress in the macaque mandible. American Journal of Physical Anthropology 112: 553–574.

Doblaré, M., García, J. M. & Gómez, M. J. (2004): Modelling bone tissue fracture and healing: a review. Engineering Fracture Mechanics 71: 1809–1840.

Dumont, E. R., Davis, J. L., Grosse, I. R. & Burrows, A. M. (2011): Finite Element Analysis of performance in the skulls of marmosets and tamarins. Journal of Anatomy 218: 151–162.

Dumont, E. R., Grosse, I. R. & Slater, G. J. (2009): Requirements for comparing the performance of finite element models of biological structures. Journal of Theoretical Biology 256: 96–103.

Early, M., Lally, C., Prendergast, P. J & Kelly, D. J. (2009): Stresses in peripheral arteries following stent placement: A Finite Element Analysis. Computer Methods in Biomechanics and Biomedical Engineering 12: 25–33.

Farke, A. A. (2008): Frontal sinuses and head-butting in goats: a Finite Element Analysis. Journal of Experimental Biology 211: 3085–3094.

Figueirido, B., Lautenschlager, S., Pérez-Ramos, A. & Van Valkenburgh, B. (2018): Distinct predatory behaviors in scimitar- and dirk-toothed sabertooth cats. Current Biology 28: 3260–3266

Figueirido, B., Tseng, Z. J., Serrano-Alarcon, F. J., Martin-Serra, A., Pastor, J. F. F., Serrano-Alarcón, F. J. & Martín-Serra, A. (2014): Three-dimensional computer simulations of feeding behaviour in red and giant pandas relate skull biomechanics with dietary niche partitioning. Biology Letters 10: 20140196

Fish, J. F. & Stayton, C. T. (2014): Morphological and mechanical changes in juvenile red-eared slider turtle (*Trachemys scripta elegans*) shells during ontogeny. Journal of Morphology 275: 391–397.

Fitton, L. C., Prôa, M., Rowland, C., Toro-Ibacache, V. & O'Higgins, P. (2015): The impact of simplifications on the performance of a Finite Element model of a *Macaca fascicularis* cranium. Anatomical Record 298: 107–121.

Fletcher, T. M., Janis, C. M. & Rayfield, E. J. (2010): Finite Element Analysis of ungulate jaws: Can mode of digestive physiology be determined? Palaeontologica Electronia 13, 3; 21A: 15 p. http://palaeo-electronica.org/2010_3/234/index.html

Fortuny, J., Marcé-Nogué, J., de Esteban-Trivigno, S., Gil, L. & Galobart, Á. (2011): Temnospondyli bite club: ecomorphological patterns of the most diverse group of early tetrapods. Journal of Evolutionary Biology 24: 2040–2054.

Fortuny, J., Marcé-Nogué, J., Gil, L. L. L & Galobart, À. (2012): Skull mechanics and the evolutionary patterns of the otic notch closure in capitosaurs (Amphibia: Temnospondyli). Anatomical Record 295: 1134–1146.

Fortuny, J., Marcé-Nogué, J., Heiss, E., Sanchez, M., Gil, L. & Galobart, À. (2015): 3D bite modeling and feeding mechanics of the largest living amphibian, the Chinese giant salamander *Andrias davidianus* (Amphibia: Urodela): PLoS One 10: e0121885.

Fortuny, J., Marcé-Nogué, J., Steyer, J.-S., de Esteban-Trivigno, S., Mujal, E. & Gil, L. (2016): Comparative 3D analyses and palaeoecology of giant early amphibians (Temnospondyli: Stereospondyli): Scientific Reports 6: 30387.

Freeman, P. W. (1979): Specialized insectivory: Beetle-eating and moth-eating molossid bats. Journal of Mammalogy 60: 467–479.

Freeman, P. W. (1981): Correspondence of food habits and morphology in insectivorous bats. Journal of Mammalogy 62: 166–173.

Freeman, P. W. (1984): Functional cranial analysis of large animalivorous bats (Microchiroptera). Biological Journal of the Linnean Society 21: 387–408.

Freeman, P. W. (1988): Frugivorous and animalivorous bats (Microchiroptera): Dental and cranial adaptations. Biological Journal of the Linnean Society 33: 249–272.

Freeman, P. W. (2000): Macroevolution in Microchiropteria: Recoupling morphology and ecology with phylogeny. Evolutionary Ecology Research 2: 317–335.

Gil, L., Marcé-Nogué, J. & Sánchez, M. (2015): Insights into the controversy over materials data for the comparison of biomechanical performance in vertebrates. Palaeontologia Electronica 18.1.10A: 1-24. https://doi.org/10.26879/509

Gill, P. G., Purnell, M. A., Crumpton, N., Brown, K. R., Gostling, N. J., Stampanoni, M. & Rayfield, E. J. (2014): Dietary specializations and diversity in feeding ecology of the earliest stem mammals. Nature 512: 303–305.

Gislason, M. K., Foster, E., Bransby-Zachary, M. & Nash, D. H. (2017): Biomechanical analysis of the Universal 2 implant in total wrist arthroplasty: A Finite Element study. Computer Methods in Biomechanics and Biomedical Engineering 20: 1113–1121.

Greaves, W. S. (1978): The jaw lever system in ungulates: a new model. Journal of Zoology 184: 271–285.

Gröning, F., Bright, J. A., Fagan, M. J. & O'Higgins, P. (2012a): Improving the validation of finite element models with quantitative full-field strain comparisons. Journal of Biomechanics 45: 1498–1506.

Gröning, F., Fagan, M. J. & O'Higgins, P. (2011a): The effects of the periodontal ligament on mandibular stiffness: A study combining Finite Element Analysis and Geometric Morphometrics. Journal of Biomechanics 44: 1304–1312.

Gröning, F., Fagan, M. & O'Higgins, P. (2012b): Modelling the human mandible under masticatory loads: Which input variables are important? Anatomical Record 295: 853–863.

Gröning, F., Fagan, M. J. & O'Higgins, P. (2013): Comparing the distribution of strains with the distribution of bone tissue in a human mandible: A Finite Element study. Anatomical Record 296: 9–18.

Gröning, F., Liu, J., Fagan, M. J. & O'Higgins, P. (2011b): Why do humans have chins? Testing the mechanical significance of modern human symphyseal morphology with Finite Element Analysis. American Journal of Physical Anthropology 144: 593–606.

Hogue, A. S. (2008): Mandibular corpus form and its functional significance: Evidence from marsupials. In: Vinyard, C., Ravosa, M. & Wall, C. (eds.). Primate Craniofacial Function and Biology. Springer Academic Publishers, New York: 329–356

Hogue, A. S. & Ravosa, M. J. (2001): Transverse masticatory movements, occlusal orientation, and symphyseal fusion in selenodont artiodactyls. Journal of Morphology 249: 221–241.

Kardong, K. V. (2014): Vertebrates: Comparative Anatomy, Function, Evolution. Open University Press, London.

Kupczik, K. (2008): Virtual biomechanics: Basic concepts and technical aspects of Finite Element Analysis in vertebrate morphology. Journal of Anthropological Sciences 86: 193–198.

Lautenschlager, S. (2016): Reconstructing the past: Methods and techniques for the digital restoration of fossils. Royal Society Open Science 3: 160342.

Lautenschlager, S., Brassey, C. A., Button, D. J. & Barrett, P. M. (2016): Decoupled form and function in disparate herbivorous dinosaur clades. Scientific Reports 6: 26495.

Lautenschlager, S., Gill, P. G., Luo, Z.-X., Fagan, M. J. & Rayfield, E. J. (2018): The role of miniaturization in the evolution of the mammalian jaw and middle ear. Nature 561: 533–537.

Ledogar, J. A., Smith, A. L., Benazzi, S., Weber, G. W., Spencer, M. A., Carlson, K. B., McNulty, K. P., Dechow, P. C., Grosse, I. R., Ross, C. F., Richmond, B. G., Wright, B. W., Wang, Q., Byron, C., Carlson, K. J., de Ruiter, D. J., Berger, L. R., Tamvada, K., Pryor, L. C., Berthaume, M. A. & Strait, D. S. (2016): Mechanical evidence that *Australopithecus sediba* was limited in its ability to eat hard foods. Nature Communications 7: 10596.

Maiorino, L., Farke, A. A., Kotsakis, T., Teresi, L. & Piras, P. (2015): Variation in the shape and mechanical performance of the lower jaws in ceratopsid dinosaurs (Ornithischia, Ceratopsia): Journal of Anatomy 227: 631–646.

Marcé-Nogué, J., de Esteban-Trivigno, S., Escrig, C. & Gil, L. (2016): Accounting for differences in element size and homogeneity when comparing Finite Element models: Armadillos as a case study. Palaeontologia Electronica 19: 1–22.

*Marcé-Nogué, J., de Esteban-Trivigno, S., Püschel, T. A. & Fortuny, J. (2017a): The intervals method: a new approach to analyse finite element outputs using multivariate statistics. PeerJ 5: e3793.

Marcé-Nogué, J., DeMiguel, D., Fortuny, J., de Esteban-Trivigno, S. & Gil, L. (2013): Quasi-homothetic transformation for comparing the mechanical performance of planar models in biological research. Palaeontologia Electronica 16, 3: 1–15. https://doi.10.26879/365

Marcé-Nogué, J., Fortuny, J., de Esteban-Trivigno, S., Sánchez, M., Gil, L .& Galobart, À. (2015): 3D computational mechanics elucidate the evolutionary implications of orbit position and size diversity of early amphibians. PLoS One 10: e0131320.

Marcé-Nogué, J., Fortuny, J., Gil, L. & Galobart, A. (2011): Using reverse engineering to reconstruct tetrapod skulls and analyse its feeding behaviour. In: Topping, B. H. V. & Tsompanakis, Y. (eds.). Proceedings of the 13th International Conference on Civil, Structural and Environmental Engineering Computing. Civil-Comp Press, Stirlingshire. https://doi.10.4203/ccp.96.237

Marcé-Nogué, J., Fortuny, J., Gil, L. & Sánchez, M. (2015): Improving mesh generation in Finite Element Analysis for functional morphology approaches. Spanish Journal of Palaeontology 31: 117–132.

*Marcé-Nogué, J., Püschel, T. A, Daasch, A. & Kaiser, T. M. (2020): Broad-scale morpho-functional traits of the mandible suggest no hard food adaptation in the hominin lineage. Scientific Reports 10: 6793.

*Marcé-Nogué, J., Püschel, T. A. & Kaiser, T. M. (2017b): A biomechanical approach to understand the ecomorphological relationship between primate mandibles and diet. Scientific Reports 7: 8364.

Marinescu, R., Daegling, D. J. & Rapoff, A. J. (2005): Finite-element modeling of the anthropoid mandible: The effects of altered boundary conditions. Anatomical Record 283: 300–309.

Mase, G. E. & Mase, G. T. (1999): Continuum Mechanics for Engineers. CRC Press, New York.

Maynard-Smith, J. & Savage, R. (1959): The mechanics of mammalian jaws. School Science Review 289–301.

McHenry, C. R., Wroe, S., Clausen, P. D., Moreno, K. & Cunningham, E. (2007): Supermodeled sabercat, predatory behavior in *Smilodon fatalis* revealed by high-resolution 3D computer simulation. Proceedings of the National Academy of Sciences of the United States of America 104: 16010–16015.

Meers, M. B. (2003): Maximum bite force and prey size of *Tyrannosaurus rex* and their relationships to the inference of feeding behavior. Historical Biology 16: 1–12.

Morris, A. (2008): A Practical Guide to Reliable Finite Element Modelling. John Wiley & Sons, Chichester.

Nalla, R. K., Kinney, J. H. & Ritchie, R. O. (2003): Mechanistic fracture criteria for the failure of human cortical bone. Nature Materials 2: 164–168.

Neenan, J. M., Ruta, M., Clack, J. A. & Rayfield, E. J. (2014): Feeding biomechanics in *Acanthostega* and across the fish-tetrapod transition. Proceedings of the Royal Society B 281: 20132689

Oldfield, C. C., McHenry, C. R., Clausen, P. D., Chamoli, U., Parr, W. C. H., Stynder, D. D. & Wroe, S. (2012): Finite Element Analysis of ursid cranial mechanics and the prediction of feeding behaviour in the extinct giant *Agriotherium africanum*. Journal of Zoology 286: 171–179.

Osborn, J. W. (1987): Relationship between the mandibular condyle and the occlusal plane during hominid evolution: Some of its effects on jaw mechanics. American Journal of Physical Anthropology 73: 193–207.

Panagiotopoulou, O., Iriarte-Diaz, J., Wilshin, S., Dechow, P. C., Taylor, A. B., Mehari Abraha, H., Aljunid, S .F. & Ross, C. F. (2017): In vivo bone strain and finite element modeling of a rhesus macaque mandible during mastication. Zoology 124: 13–29.

Parr, W. C. H., Wroe, S., Chamoli, U., Richards, H. S., McCurry, M. R., Clausen, P. D & McHenry, C. R. (2012): Toward integration of Geometric Morphometrics and computational biomechanics: New methods for 3D virtual reconstruction and quantitative analysis of Finite Element models. Journal of Theoretical Biology 301: 1–14.

Piras, P., Maiorino, L., Teresi, L., Meloro, C., Lucci, F., Kotsakis, T. & Raia, P. (2013): Bite of the cats: Relationships between functional integration and mechanical performance as revealed by mandible geometry. Systematic Biology 62: 878–900.

Piras, P., Sansalone, G., Teresi, L., Moscato, M., Profico, A., Eng, R., Kotsakis, T. (2015): Digging adaptation in insectivorous subterranean eutherians. The enigma of *Mesoscalops montanensis* unveiled by Geometric Morphometrics and Finite Element Analysis. Journal of Morphology 276: 1157–1171.

Porro, L. B., Holliday, C. M., Anapol, F., Ontiveros, L. C. L. T. & Ross, C. F. (2011): Free body analysis, beam mechanics, and finite element modeling of the mandible of *Alligator mississippiensis*. Journal of Morphology 272: 910–937.

Preuschoft, H. & Witzel, U. (2002): Biomechanical investigations on the skulls of reptiles and mammals. Senckenbergiana lethaea 82: 207–222.

Püschel, T. A. & Sellers, W. I. (2016): Standing on the shoulders of apes: Analyzing the form and function of the hominoid scapula using Geometric Morphometrics and Finite Element Analysis. American Journal of Physical Anthropology 159: 325–341.

Püschel, T. A., Marcé-Nogué, J., Gladman, J. T., Bobe, R. & Sellers, W. I. (2018): Inferring locomotor behaviours in Miocene New World monkeys using Finite Element Analysis, Geometric Morphometrics and machine-learning classification techniques applied to talar morphology. Journal of The Royal Society Interface 15: 20180520.

*Püschel, T. A., Marcé-Nogué, J., Kaiser, T. M., Brocklehurst, R. J. & Sellers, W. I. (2018): Analyzing the sclerocarpy adaptations of the Pitheciidae mandible. American Journal of Primatology 80: e22759.

Qian, L., Todo, M., Morita, Y., Matsushita, Y. & Koyano, K. (2009): Deformation analysis of the periodontium considering the viscoelasticity of the periodontal ligament. Dental Materials 25: 1285–1292.

Radinsky, L. B. (1981a): Evolution of skull shape in carnivores: 2. Additional modern carnivores. Biological Journal of the Linnean Society 16: 337–355.

Radinsky, L. B. (1981b): Evolution of skull shape in carnivores 1. Representative modern carnivores. Biological Journal of the Linnean Society 15: 369–388.

Rahman, I. A. & Lautenschlager, S. (2016): Applications of three-dimensional box modeling to paleontological functional analysis. The Paleontological Society Papers 22: 119–132.

Rayfield, E. J. (2007): Finite Element analysis and understanding the biomechanics and evolution of living and fossil organisms. Annual Review of Earth and Planetary Sciences 35: 541–576.

Richard, A. F., Goldstein, S. J. & Dewar, R. E. (1989): Weed macaques: The evolutionary implications of macaque feeding ecology. International Journal of Primatology 10: 569–594.

Ross, C. F. & Iriarte-Diaz, J. (2014): What does feeding system morphology tell us about feeding? Evolutionary Anthropology 23: 105–120.

Ross, C. F., Iriarte-Diaz, J. & Nunn, C. L. (2012): Innovative approaches to the relationship between diet and mandibular morphology in primates. International Journal of Primatology 33: 632–660.

Sella-Tunis, T., Pokhojaev, A., Sarig, R., O'Higgins, P. & May, H. (2018): Human mandibular shape is associated with masticatory muscle force. Scientific Reports 8: 1–10.

Sellers, K. C., Middleton, K. M., Davis, J. L. & Holliday, C. M. (2017): Ontogeny of bite force in a validated biomechanical model of the American alligator. Journal of Experimental Biology 220: 2036–2046.

Serrano-Fochs, S., de Esteban-Trivigno, S., Marcé-Nogué, J., Fortuny, J. & Fariña, R. A. (2015): Finite Element Analysis of the Cingulata jaw: An ecomorphological approach to armadillo's diets. PLoS One 10: e0120653.

Snively, E., Fahlke, J. M. & Welsh, R. C. (2015): Bone-breaking bite force of *Basilosaurus isis* (Mammalia, Cetacea) from the Late Eocene of Egypt estimated by Finite Element Analysis. PLoS One 10: e0118380.

Spencer, L. M. (1995): Morphological correlates of dietary resource partitioning in the African Bovidae. Journal of Mammalogy 76: 448–471.

Spencer, M. A. (1999): Constraints on masticatory system evolution in anthropoid primates. American Journal of Physical Anthropology 108: 483–506.

Strait, D. S., Constantino, P. J., Lucas, P. W., Richmond, B. G., Spencer, M. A., Dechow, P. C., Ledogar, J. A. (2013): Viewpoints: Diet and dietary adaptations in early hominins: The hard food perspective. American Journal of Physical Anthropology 151: 339–355.

Taylor, A. B. (2006): Feeding behavior, diet, and the functional consequences of jaw form in orangutans, with implications for the evolution of *Pongo*. Journal of Human Evolution 50: 377–393.

Thomason, J. J. (1991): Cranial strength in relation to estimated biting forces in some mammals. Canadian Journal of Zoology 69: 2326–2333.

Timoshenko, S. (1955): Strength of Materials. Van Nostrand, New York.

Tseng, Z. J. (2009): Cranial function in a late Miocene *Dinocrocuta gigantea* (Mammalia: Carnivora) revealed by comparative Finite Element Analysis. Biological Journal of the Linnean Society 96: 51–67.

Tseng, Z. J. (2013): Testing adaptive hypotheses of convergence with functional landscapes: A case study of bone-cracking hypercarnivores. PLoS One 8: e65305.

Tseng, Z. J. & Binder, W. J. (2010): Mandibular biomechanics of *Crocuta crocuta*, *Canis lupus*, and the late Miocene *Dinocrocuta gigantea* (Carnivora, Mammalia): Zoological Journal of the Linnean Society 158: 683–696.

Tseng, Z. J . & Flynn, J. J. (2015): Convergence analysis of a Finite Element skull model of *Herpestes javanicus* (Carnivora, Mammalia): Implications for robust comparative inferences of biomechanical function. Journal of Theoretical Biology 365: 112–148.

Tseng, Z. J. & Flynn, J. J. (2018): Structure-function covariation with nonfeeding ecological variables influences evolution of feeding specialization in Carnivora. Science Advances: 4: eaao5441.

Tseng, Z. J., Grohé, C. & Flynn, J. J. (2016): A unique feeding strategy of the extinct marine mammal *Kolponomos*: convergence on sabretooths and sea otters. Proceedings of the Royal Society B 283: 20160044.

Tseng, Z. J., Su, D. F., Wang, X., White, S. C. & Ji, X. (2017): Feeding capability in the extinct giant *Siamogale melilutra* and comparative mandibular biomechanics of living Lutrinae. Scientific Reports 7: 15225.

van Eijden, T. M. (2000): Biomechanics of the mandible. Critical Reviews in Oral Biology & Medicine 11: 123–136.

Varela, L. & Fariña, R. A. (2015): Masseter moment arm as a dietary proxy in herbivorous ungulates. Journal of Zoology 296: 295–304.

Veitschegger, K., Wilson, L. A. B., Nussberger, B., Camenisch, G., Keller, L. F., Wroe, S. & Sánchez-Villagra, M. R. (2018): Resurrecting Darwin's Niata – anatomical, biomechanical, genetic, and morphometric studies of morphological novelty in cattle. Scientific Reports 8: 9129.

Vizcaíno, S. F., Bargo, M. S., Cassini, G. H. & Toledo, N. (2016): Forma y función en paleobiología de vertebrados. Editorial de la Universidad Nacional de La Plata, La Plata.

Walmsley, C. W., Smits, P. D., Quayle, M. R., McCurry, M. R., Richards, H. S., Oldfield, C. C. & McHenry, C. R. (2013): Why the long face? The mechanics of mandibular symphysis proportions in crocodiles. PLoS One 8: e53873.

Wroe, S., Chamoli, U., Parr, W. C. H., Clausen, P. D., Ridgely, R. & Witmer, L. M. (2013): Comparative biomechanical modeling of metatherian and placental saber-tooths: A different kind of bite for an extreme pouched predator. PLoS One 8: e66888

Wroe, S., Clausen, P. D., McHenry, C. R., Moreno, K. & Cunningham, E. (2007): Computer simulation of feeding behaviour in the thylacine and dingo as a novel test for convergence

and niche overlap. Proceedings of the Royal Society B 274: 2819–2828.

Wroe, S., Ferrara, T. L., McHenry, C. R., Curnoe, D. & Chamoli, U. (2010): The craniomandibular mechanics of being human. Proceedings of the Royal Society B 277: 3579–3586.

Wroe, S., McHenry, C. R & Thomason, J. J. (2005): Bite club: comparative bite force in big biting mammals and the prediction of predatory behaviour in fossil taxa. Proceedings of the Royal Society B 272: 619–625.

*Zhou, Z., Winkler, D. E., Fortuny, J., Kaiser, T. M. & Marcé-Nogué, J. (2019): Why ruminating ungulates chew sloppily: Biomechanics discern a phylogenetic pattern. PLoS One 14: e0214510.

Zienkiewicz, O. C. & Taylor, R. L. (2000): Finite Element Method – The Basis (Vol. 1). Butterworth-Heinemann, Oxford.